AD-A160 061 INDEPENDENT RESEARCH AND DEVELOPMENT: INFRARED SENSOR TECHNOLOGY PROGRAM..(U) JOHNS HOPKINS UNIV LAUREL MD APPLIED PHYSICS LAB R W BRUNS ET AL. MAY 85 1/1

UNCLASSIFIED JHU/APL/TG-1349 N00024-85-C-5301 F/G 17/3 NL

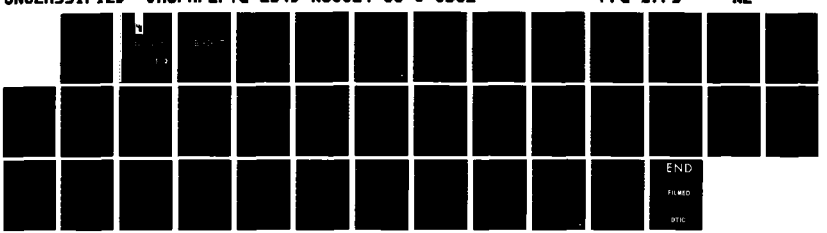

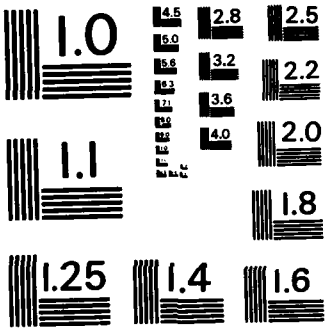


MICROCOPY RESOLUTION TEST CHART
NATIONAL BUREAU OF STANDARDS - 1963 - A

JHU/APL
TG 1349
MAY 1985
Copy No.

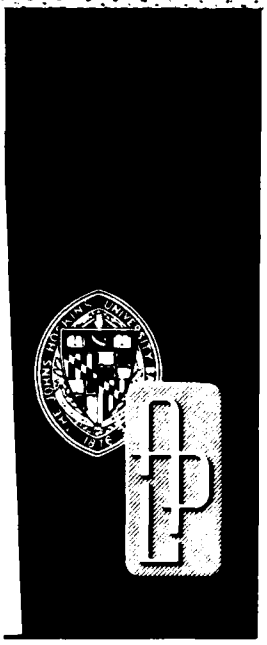

(12)

*Technical Memorandum*

# INDEPENDENT RESEARCH AND DEVELOPMENT: INFRARED SENSOR TECHNOLOGY PROGRAM TEST PLAN

R. W. BRUNS, J. H. PANESCI,
W. J. TROPF, and L. B. WECKESSER





THE JOHNS HOPKINS UNIVERSITY ■ APPLIED PHYSICS LABORATORY

JHU/APL
TG 1349
MAY 1985

*Technical Memorandum*

# INDEPENDENT RESEARCH AND DEVELOPMENT: INFRARED SENSOR TECHNOLOGY PROGRAM TEST PLAN

R. W. BRUNS, J. H. PANESCI,
W. J. TROPF, and L. B. WECKESSER

THE JOHNS HOPKINS UNIVERSITY ■ APPLIED PHYSICS LABORATORY
Johns Hopkins Road, Laurel, Maryland 20707
Operating under Contract N00024-85-C-5301 with the Department of the Navy

UNCLASSIFIED
SECURITY CLASSIFICATION OF THIS PAGE

AD-A160 061

# REPORT DOCUMENTATION PAGE

| | |
|---|---|
| 1a. REPORT SECURITY CLASSIFICATION<br>Unclassified | 1b. RESTRICTIVE MARKINGS |
| 2a. SECURITY CLASSIFICATION AUTHORITY | 3. DISTRIBUTION/AVAILABILITY OF REPORT<br>Approved for public release; distribution is unlimited |
| 2b. DECLASSIFICATION/DOWNGRADING SCHEDULE<br>n/a | |
| 4. PERFORMING ORGANIZATION NUMBER(S)<br>JHU/APL TG 1349 | 5. MONITORING ORGANIZATION REPORT NUMBER(S)<br>JHU/APL TG 1349 |
| 6a. NAME OF PERFORMING ORGANIZATION<br>The Johns Hopkins University Applied Physics Laboratory | 6b. OFFICE SYMBOL (*If Applicable*)<br>F1F |
| 7a. NAME OF MONITORING ORGANIZATION<br>NAVPRO, Laurel, Maryland | |
| 6c. ADDRESS (*City, State, and ZIP Code*)<br>Johns Hopkins Road<br>Laurel, Maryland 20707 | 7b. ADDRESS (*City, State, and ZIP Code*)<br>Johns Hopkins Road<br>Laurel, Maryland 20707 |
| 8a. NAME OF FUNDING/SPONSORING ORGANIZATION<br>JHU/APL Independent Research and Development Program | 8b. OFFICE SYMBOL (*If Applicable*)<br>F1 |
| 9. PROCUREMENT INSTRUMENT IDENTIFICATION NUMBER<br>N00024-85-C-5301 | |
| 8c. ADDRESS (*City, State, and ZIP Code*)<br>Johns Hopkins Road<br>Laurel, Maryland 20707 | 10. SOURCE OF FUNDING NUMBERS<br>PROGRAM ELEMENT NO. / PROJECT NO. / TASK NO. X8G5 / WORK UNIT ACCESSION NO. |

11. TITLE (*Include Security Classification*)

Independent Research and Development: Infrared Sensor Technology Program Test Plan

12. PERSONAL AUTHOR(S)

R. W. Bruns, J. H. Panesci, W. J. Tropf, and L. B. Weckesser

| 13a. TYPE OF REPORT | 13b. TIME COVERED | 14. DATE OF REPORT (*Year, Month, Day*) | 15. PAGE COUNT |
|---|---|---|---|
| Technical Memorandum | FROM _____ TO _____ | May 1985 | 38 |

16. SUPPLEMENTARY NOTATION

| 17. COSATI CODES | | | 18. SUBJECT TERMS |
|---|---|---|---|
| FIELD | GROUP | SUB-GROUP | ~~advanced guidance~~ free-jet facility; guidance technology; heat transfer; ~~high-speed flight~~ infrared guidance; infrared sensors; optical distortion; optical testing; ~~test plan~~ thermal testing. |
| | | | |
| | | | |

19. ABSTRACT (*Continue on reverse if necessary and identify by block number*)

Infrared (IR) sensors will provide significant performance improvements for advanced guided missiles. The use of IR guidance in high-performance, endoatmospheric missiles requires basic research and technology development to ensure survival and adequate performance in the high-temperature environment of high-speed flight. To gain a fundamental understanding of the performance of IR sensors in high thermal conditions, The Johns Hopkins University Applied Physics Laboratory initiated an Infrared Sensor Technology Program as an Independent Research and Development Task. The technology program combines development of both an analytical and an experimental capability to answer fundamental feasibility questions, to gather basic data, and to develop the capability to evaluate performance over all flight regimes. This test plan describes the experimental work to be conducted during 1985. Included are descriptions of the principal test facility, measurement instrumentation, and data recording used in the program. Aerothermal and optical performance measurements will be made on a test article (model) with an uncooled, hemispherical window. Mach 5 flow and heat-transfer rates representative of flight speeds from Mach 5 to Mach 6.5 and altitudes from 50,000 to 100,000 ft will be used. Test conditions, measurements, and data reporting are described.

| 20. DISTRIBUTION/AVAILABILITY OF ABSTRACT | 21. ABSTRACT SECURITY CLASSIFICATION |
|---|---|
| ☐ UNCLASSIFIED/UNLIMITED ☒ SAME AS RPT. ☐ DTIC USERS | Unclassified |
| 22a. NAME OF RESPONSIBLE INDIVIDUAL<br>Robert W. Irvin | 22b. TELEPHONE (*Include Area Code*)<br>(301) 953-5403 / 22c. OFFICE SYMBOL<br>SE |

DD FORM 1473, 84 MAR

SECURITY CLASSIFICATION OF THIS PAGE
UNCLASSIFIED

THE JOHNS HOPKINS UNIVERSITY
APPLIED PHYSICS LABORATORY
LAUREL, MARYLAND

## ABSTRACT

Infrared (IR) sensors will provide significant performance improvements for advanced guided missiles. The use of IR guidance in high-performance, endoatmospheric missiles requires basic research and technology development to ensure survival and adequate performance in the high-temperature environment of high-speed flight. To gain a fundamental understanding of the performance of IR sensors in high thermal conditions, The Johns Hopkins University Applied Physics Laboratory initiated an Infrared Sensor Technology Program as an Independent Research and Development task.

The technology program combines development of both an analytical and an experimental capability to answer fundamental feasibility questions, to gather basic data, and to develop the capability to evaluate performance over all flight regimes. This test plan describes the experimental work to be conducted during 1985. Included are descriptions of the principal test facility, measurement instrumentation, and data recording used in the program. Aerothermal and optical performance measurements will be made on a test article (model) with an uncooled, hemispherical window. Mach 5 flow and heat-transfer rates representative of flight speeds from Mach 5 to Mach 6.5 and altitudes from 50,000 to 100,000 ft will be used. Test conditions, measurements, and data reporting are described.



# CONTENTS

**List of Illustrations** ..... 6

**List of Tables** ..... 6

**1.0 Introduction** ..... 7
1.1 Background ..... 7
1.2 Program Objectives ..... 7
1.3 Scope ..... 8
1.4 Summary ..... 8

**2.0 Test Facilities** ..... 8
2.1 Propulsion Research Facility ..... 8
2.2 IR Seeker Aerothermal Test Facility ..... 8
2.3 IR Signal Injector ..... 10
2.4 Test Cabin ..... 11
2.5 Test Article ..... 12
2.6 Test Instrumentation ..... 13
2.6.1 Facility Monitoring and Control Instrumentation ..... 14
2.6.2 Optical Target Projection Instrumentation ..... 14
2.6.3 Pressure and Calorimetry Instrumentation ..... 18
2.6.4 Thermostructural Instrumentation of the Infrared Window ..... 18
2.6.5 Optical Instrumentation ..... 21

**3.0 Test Descriptions** ..... 23
3.1 Facility Checkout and Capability Measurements ..... 23
3.1.1 Facility Flow Field Tests ..... 23
3.1.2 Facility Turbulence and Vibration Measurements ..... 24
3.1.3 Flow IR Transmission Measurements ..... 25
3.2 IR Seeker Test Condition Matrix ..... 26
3.3 Test-Article Measurements ..... 28
3.3.1 Pressure and Calorimetry Measurements ..... 28
3.3.2 Window Thermostructural Measurements ..... 28
3.3.3 Optical Measurements ..... 29
3.4 Data Recording and Facility Control ..... 30
3.5 Data Reduction and Reporting ..... 32

**4.0 Test Schedule** ..... 33

**Appendix A: Test Function Symbol Nomenclature** ..... 35

**Appexdix B: Typical Test Sequence** ..... 35

# ILLUSTRATIONS

1. IR Seeker Aerothermal Test Facility ..... 9
2. Conditions simulated by the IR Seeker Aerothermal Test Facility ..... 10
3. Top view of the IR signal injector and the target projection optics ..... 11
4. Test cabin configuration showing test article insertion ..... 12
5. Test article in optical testing configuration ..... 13
6. Calibration dome for facility pressure and calorimetry measurements ..... 20
7. Facility operating conditions for 530°R incoming air, showing initial flow-field measurement conditions ..... 24
8. Facility operating conditions for 1500°R incoming air ..... 25
9. PRL instrumentation and control system for automated testing in the IR Seeker Aerothermal Test Facility ..... 32

# TABLES

1. Control and monitoring instrumentation for the IR Seeker Aerothermal Test Facility ..... 15
2. Target projection and test-article optical instrumentation ..... 19
3. Pressure and calorimetry instrumentation ..... 21
4. Thermostructural instrumentation ..... 21
5. Test matrix for the IR Seeker Aerothermal Facility ..... 27
6. Parameters for evaluation of the optical performance of High-Speed IR Seekers ..... 29
7. Data acquisition capabilities of PRL ..... 31
8. 1985 testing schedule for IR Seekers ..... 34

# 1.0 INTRODUCTION

## 1.1 Background

Advanced guided missiles must cope with an array of high-performance air targets that present unique guidance problems. The future threat will include high-speed targets, high-altitude targets, targets with very low radar cross section, targets screened by standoff countermeasures, and tightly-grouped or formation targets. Infrared (IR) guidance is a highly promising solution to all of these stressing target attributes. The characteristics of IR guidance that meet future missile-guidance needs are the high angular resolution, low noise and fast response, and target signature attributes.

The high spatial resolution provides a means of resolving closely-spaced air targets such as aircraft in formation, as well as an added means of discrimination to counter off-axis standoff jammers, multiple blinking targets, and targets that employ monopulse countermeasures against radar guidance. The combination of low noise and fast guidance response offers a combination of shorter homing time, better response against maneuvering targets, and reduced miss distance against all classes of targets. IR signatures have two particularly significant characteristics: the signature grows rapidly with target speed and it is not amenable to significant reductions. These characteristics make IR guidance a highly desirable or necessary mode for many advanced missile applications, either as a primary guidance mode or in a dual-mode radar and IR sensor combination.

Advanced antiair guided missiles will also travel at significantly higher speed or for significantly longer flight times (or both) when compared to current weapons. The high temperatures and long thermal soak times resulting from these missile performance improvements will be extremely stressing on the all of the missile subsystems. Guidance, the most complex of the missile functions, is particularly affected by the flight thermal environment. Moreover, IR guidance, heretofore used only in short-range, lower-speed missiles and employing a thermal detection technique, requires significant development before application in advanced missiles can be achieved. Hence IR guidance is rightly considered a high risk for high-speed application.

In recognition of the significant need and high payoff of IR guidance, coupled with relative immaturity of IR sensor technology for advanced, high-performance guided missiles, the Applied Physics Laboratory established the Infrared Sensor Technology Program in 1985. This program is a combined analytical and experimental effort to develop advanced IR sensors for future missiles. Test Cell number four of the APL Propulsion Research Laboratory is dedicated to measuring the characteristics and performance of IR guidance in high-speed flight conditions. This new capability is called the IR Seeker Aerothermal Test Facility.

## 1.2 PROGRAM OBJECTIVES

The overall objective of the Infrared Sensor Technology Program is to advance IR technology toward application on advanced guided missiles. Technology advances include development of analytic tools and an empirical database that supports both design and performance evaluation of IR guidance for high-speed missiles. The results of analysis and experiments will be compared to validate the analytical tools, to assess the experimental techniques, and to provide empirical data where needed. Capabilities developed by this IR program will be applied to determine the performance limits of particular sensor concepts and to demonstrate feasibility and performance of these concepts in limited 'proof-of-principle' demonstrations.

A major portion of the first-year effort of the program is to develop the required test capability. The test facility must be capable of realistically simulating the flow, and the aerothermal and optical environments of high-speed flight and must incorporate specialized instrumentation to make the unique measurements required to support the technology development. Test facility objectives for 1985 are:

1. Develop a facility to simulate the high-speed flight environment of advanced missile concepts. Check out and characterize the facility.
2. Develop test instrumentation for making the necessary flow, aerothermal, stress, and optical measurements for sensor development.
3. Design and construct test articles for measurements and proof-of-principle testing.
4. Conduct an initial set of flow, thermal, stress, and optical measurements for instrumentation validation and comparison to analytic predictions.
5. Document facility capabilities, test instrumentation, and test results.

This report is a plan for meeting these objectives.

### 1.3 SCOPE

The plan covers the testing required to check out and calibrate the IR Seeker Aerothermal Test Facility, the development of instrumentation required for the facility monitoring and control, and the design of the test article and sensors for thermal, structural, and optical performance measurements of simulated IR seekers in high-speed flight environments. Test conditions, instrumentation, test articles, and measurements to be made are described in detail. Expected analytic results that parallel measured data are included.

In addition to this overall test plan, detailed test sequences will be prepared for individual tests. Furthermore, since the planned tests are exploratory, results may dictate that tests be repeated or may suggest new types of tests or test conditions outside the scope of this plan.

### 1.4 SUMMARY

This test plan outlines the facility, equipment, and instrumentation as well as the testing to be conducted during the first year of the Infrared Sensor Technology Program. A unique IR Seeker Aerothermal Test Facility will be developed and readied for use during the first half of 1985. The facility will be checked out, calibrated, and used to conduct a series of exploratory tests on a test article (model) representing a near-term, high-speed IR seeker concept during the second half of 1985. Flow, thermostructural, and optical measurements will be made under simulated flight conditions. These measurements will be compared to analytical results for verification and will form a database for seeker design and development. Products of the first year of the test program are establishment of a facility, use of the facility to develop measurement instrumentation and techniques, and conduct of proof-of-principle testing on the initial seeker concept.

## 2.0 TEST FACILITIES

The first-year goal of the Infrared Sensor Technology Program is to build and prove the facility and instrumentation for an initial series of IR seeker performance measurements. Here we describe the characteristics and capabilities of the facility and associated instrumentation that dictate both the test conditions and the measurements that can be made. As the program progresses, significant additions and improvements will be made to the facility and the instrumentation. The planned improvements are mentioned in the descriptions of the test facilities.

### 2.1 PROPULSION RESEARCH LABORATORY

The Propulsion Research Laboratory (PRL) is a major facility for conducting research in air-breathing propulsion and aerodynamics. This laboratory provides the basic utilities, control, and data acquisition capability to the IR Seeker Aerothermal Test Facility. PRL uses a blow-down system that provides heated, high-pressure air to the test cell where the air is further heated to a stagnation temperature that matches the desired flight condition and is accelerated to the desired flight velocity in a nozzle. For IR seeker testing, the facility will be operated in a free-jet mode. An exhauster system will be used when high-altitude conditions are simulated.

PRL has an extensive capability to monitor and control testing. A digital computer system can be used to provide automatic control of the air flow, air heating, cooling-water flow, and steam flow to the ejectors for altitude simulation (when required). The control system can be used to inject and remove the model from the flow field and provide on/off functions for cameras and other parts of the test instrumentation. Data recording is controlled by the same executive computer that controls the facility. Each test cell is connected to the control building via shielded cables, and signals can be routed to the appropriate instruments, controllers, or recorders via a plug-in patchboard.

### 2.2 IR SEEKER AEROTHERMAL TEST FACILITY

The IR Seeker Aerothermal Test Facility is specifically designed for testing advanced optical guidance systems. The basic layout of the test cell is shown in

Fig. 1. High-pressure (to 1000 psia) air from the PRL supply is either passed directly to the test cell or passed through a storage heater (1500° R at 50 lbm/sec or 2000° R at 10 lbm/sec) into the test setup. Further heating (to 4000° R) can be achieved by mixing and burning hydrogen in a water-cooled heater. Output from the heater passes into a water-cooled elbow tee (injector/mixer) that allows an IR signal to enter the system and pass through the nozzle throat to the test article located at the nozzle exit. A small amount of cold, dry air can be bled into the high-pressure side of the system to keep the optical window in the pressure vessel relatively cool and to reduce the optical path through the higher-pressure, high-water-vapor mixture generated by the hydrogen combustion process.

The high-temperature, high-pressure gas is expanded through a water-cooled, stainless steel Mach 5 nozzle. The diameter of the beryllium-copper throat section of the nozzle is 1.78 in., and the nozzle exit diameter is 10 in. The contour of the nozzle expansion section is designed to produce a uniform flow field parallel to the nozzle centerline. An alternate Mach 4 nozzle throat, capable of increasing the mass flow and therefore the range of heat-transfer conditions, is under consideration for future testing needs.

The test cabin houses the test article (or model) and includes a thermal shield to protect the test article during nozzle start up and shut down. An injection mechanism can insert the test article into the nozzle flow in less than one second to simulate the sudden exposure caused by uncovering the IR seeker during flight. This mechanism can also insert the test model at different locations in the flow field to obtain measurements at different viewing conditions. The cabin includes four 6-in. diameter optical ports for viewing the test article. Two ports face each other on opposite sides of the cabin, one is on the top above the test article, and one allows viewing of the model at 45° from the flow axis. These ports can be used for a variety of purposes such as flow visualization (Schleiren or interferometric), television recording, or optical signal injection.

The model injection mechanism is secured to a 14-ft long, 7000-lb granite optical table that is supported on an air-bearing system to decouple it from test-cell vibrations. Test-cabin vibrations are isolated from the model injection mechanism by a flexible seal that maintains pressure integrity in the cabin. Optical signal projection instrumentation for either through-the-nozzle or through-the-cabin viewing will also be mounted on the optical table.

An infrared signal to the test article is provided by a diode laser operating at 4 $\mu$m (a region of minimum water-vapor absorption). The laser output is spatially filtered, expanded, and collimated to provide a 3-in.-diameter beam. The laser output is modulated (chopped) to provide very high rejection of stray infrared radiation from the hot gases, the nozzle walls, the test-article window, and other sources. A visible helium-neon (HeNe) laser source will also be available for optical measurements. This source has the advantage that it can operate at a wavelength not significantly affected by radiation from the hot gas and heated dome.

After the flow passes through the test cabin, it enters a water-cooled diffuser. This diffuser decelerates the Mach 5 flow to subsonic velocity and raises the gas

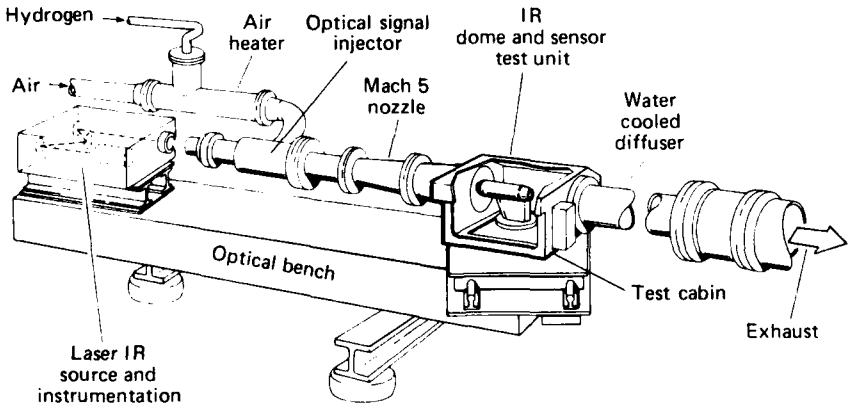


**Figure 1**—IR Seeker Aerothermal Test Facility.

pressure from the low value in the test cabin to a level that the exhaust system can handle. The gases are then cooled, scrubbed, and exhausted by steam ejectors.

A summary of test conditions that can be generated in the IR Seeker Aerothermal Test Facility are shown in Fig. 2, assuming a 2.8-in.-diameter hemispherical dome on the test article. Stagnation-point heat transfer (Q) can ma ı a wide range of test conditions, limited primarily by gas temperature and pressure (high limit) and the exhaust system (low limit). Flow temperature can be simulated to flight conditions above Mach 6 (limited by 4000° R total temperature), while the exact free-flight flow conditions can be exactly simulated only at Mach 5. The facility is capable of sustained operation for about 60 sec. at the high mass-flow and temperature conditions and greater than 10 min. at low-flow conditions. Figure 2 also shows the expanded test capability possible with the substitution of a Mach 4 throat in the nozzle.

## 2.3 IR SIGNAL INJECTOR

A unique feature of the facility is its ability to project a collimated optical beam through the nozzle throat onto the test article. This IR signal is the primary reference for optical measurements described in Section 3.3.3. Since a target is generally ahead of the missile, projection of simulated targets in the flow direction (i.e., nominal flight direction) is highly desirable. The alternative is a simulated target mounted within the free-jet nozzle or at a high oblique angle in the test cabin. A window mounted in the water-cooled nozzle will experience significant heating, will interfere with the flow of coolant, and must be large in order to project an adequate (2-in.) beam size. Any seams or joints in the interface between a nozzle-mounted window will significantly disturb the uniformity of the flow and the window would have to conform to the nozzle shape. The alternative of projecting an IR signal from the test cabin is feasible, but is limited to 45° (or greater) from the flow axis (thus only part of the desired optical data can be obtained). The test cabin will have this capability (see Section 2.4).

Implementation of a 'through-the-nozzle' signal injection system requires that the high-pressure, high-temperature flow enter the nozzle at an oblique angle from a section that has an optical window with a clear view directly through the nozzle throat to the test cabin. The layout of the injector section is shown in Fig. 3. The high temperature of the flow requires water cooling of most facility hardware. In particular, the IR signal injector section requires considerable cooling because of the large surface area exposed to stagnation conditions. Furthermore, window temperature considerations dictate that the window be thermally protected. Protection of the IR signal injection win-

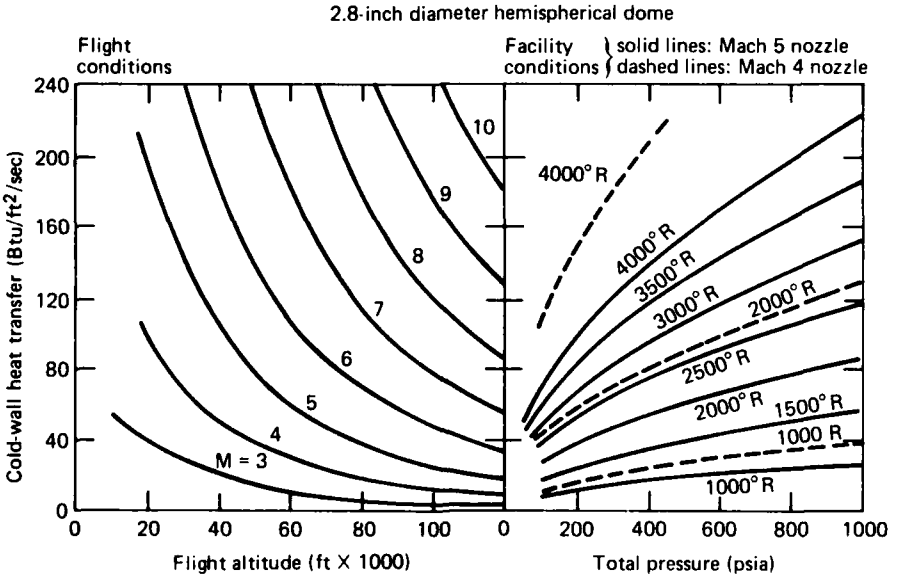


**Figure 2**—Conditions simulated by the IR Seeker Aerothermal Test Facility.

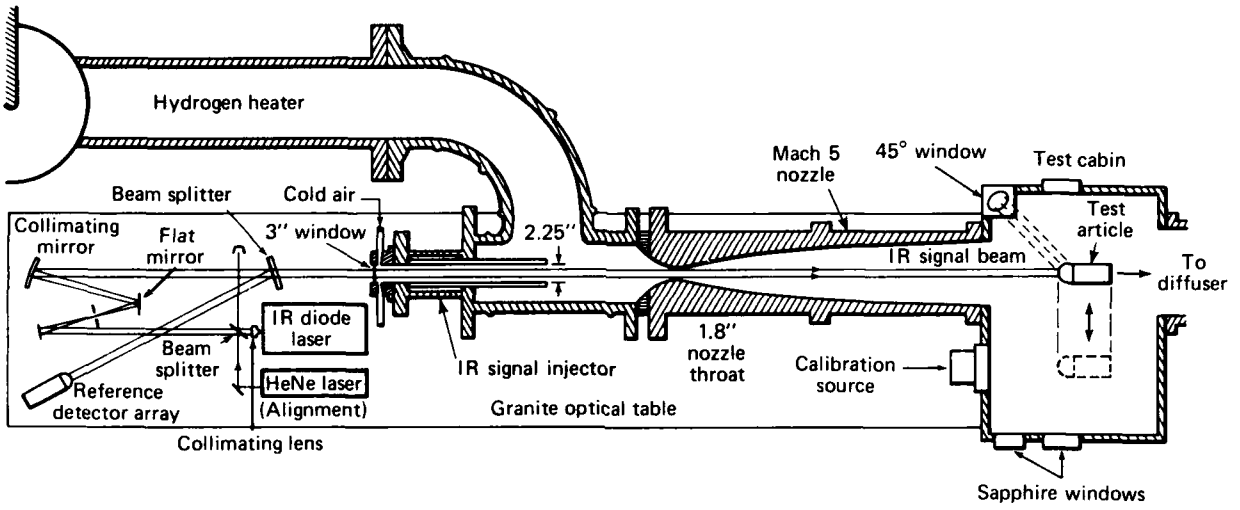


**Figure 3**—Top view of the IR signal injector and the target projection optics.

dow is accomplished by placing the window away from the main portion of the flow in a water-cooled extension of the injector. Provisions have also been made to input cool air at the window location. The need for cool air injection as well as the effect of this injection on the facility performance (including generation of optical turbulence) will be determined during facility checkout.

Windows for the IR signal injection port will have a 3-in. clear aperture. Windows of two materials have been procured: sapphire (stronger and higher temperature) and calcium fluoride (better optical properties at elevated temperature). Selection of the window to be used will depend on the results of the facility checkout measurements.

The IR signal source (see Section 2.6.2) is located on the granite optical table. This table is isolated from the rest of the facility and suspended on air-bearing legs. The test article is mounted at the other end of the granite table as described below. Relative motion between the test article (model) and the IR signal source is minimized by mounting both systems on the same granite block.

## 2.4 TEST CABIN

The test cabin, shown in Fig. 4, contains the test article that is to be exposed to simulated flight conditions. The cabin is attached to the exit plane of the nozzle, and the exhaust diffuser is attached to the rear of the cabin. The nozzle exit and diffuser entrance are on the same centerline and separated by 25 in. This space is used for testing the model. During nozzle start-up the test article is located out of the flow field behind a protective shutter. After the nozzle is started, the shutter is lifted and the test article is moved rapidly into the flow field. After exposure, the test article and shutter are returned to their starting positions before the nozzle flow is terminated.

This design and method of operation provides a number of benefits. Sudden exposure to the flight environment (simulating seeker exposure after launch) can be duplicated. Nozzle starting problems caused by test article blockage are avoided. Nozzle start-up and shut-down loads on the model and support string are eliminated. Finally, start-up procedures for air flow and heater are simplified.

The test article, holder, and sting move 17 in. in less than 1 sec. they are inserted into the flow field. They will decelerate during the final portion of travel to reduce the shock produced at the end of travel. The track used to insert the test article is normally perpendicular to the nozzle centerline, but can be rotated up to 30° from this line to change the position of the test article in the flow. The position of the front tip of the test article can be varied from slightly inside the nozzle to approximately 12 in. behind the nozzle exit. During the first series of tests, the centerline of the cylindrical test-article holder will be parallel to the flow centerline. Testing the model at an angle of attack to the flow field is under consideration, but may not be practical because of nozzle-flow breakdown and diffuser spillage. Alternatively, the test-article optics

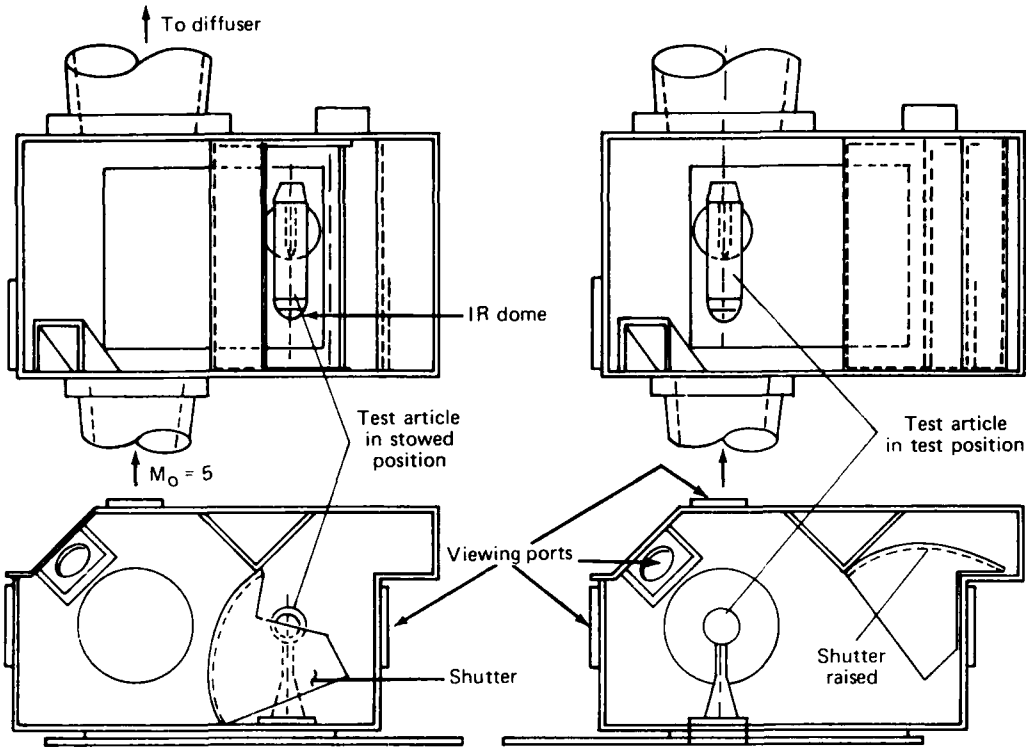


**Figure 4**—Test cabin configuration showing test article insertion.

can be modified to allow viewing at 40° to the flow, when the model is parallel to the flow. This technique will closely simulate angle of attack, from the standpoint of optical measurement.

The test article is rigidly attached to the granite table through its support sting and translating mechanism. Isolation of the model translating mechanism from facility vibration is achieved by a flexible seal between the cabin and translation system. This seal will maintain cabin-pressure integrity during testing. The cabin pressure will normally be significantly less than 1 atm.

The test article can be viewed through one of several windows attached to the test cabin. Side-mounted sapphire windows (4-in. clear aperture) allow flow visualization, remote sensing of the flow or the test article conditions (temperature, concentration, flow velocity), or viewing. Two of these windows are placed on opposite sides of the cabin; a third allows viewing at a 45° angle to the flow. This third window will be used as an alternate IR signal injection port. A fourth window of quartz (6-in. clear aperture), located above the flow field at the nozzle exit, will be used primarily for photographic recording.

When the sting is in the stowed position, access ports in the test cabin will allow checkout, calibration, and adjustment of the test article as well as removal and insertion of the test article into the holder atop the sting. Built-in optical test and calibration may be included as features of the test cabin.

## 2.5 TEST ARTICLE

It is expected that several types of test article will be used during the course of the program. The configuration described in the following paragraphs will be used in the facility checkout, and calibration, and in the initial series of tests.

The initial test article will be housed in a cylindrical, water-cooled jacket mounted atop a sting (see Figs. 4 and 5). The front of the test article will be a segment of a hemisphere, either a metal dome used for facility checkout or an optical dome (e.g., spinel) attached to an uncooled metal dome-holding ring (which

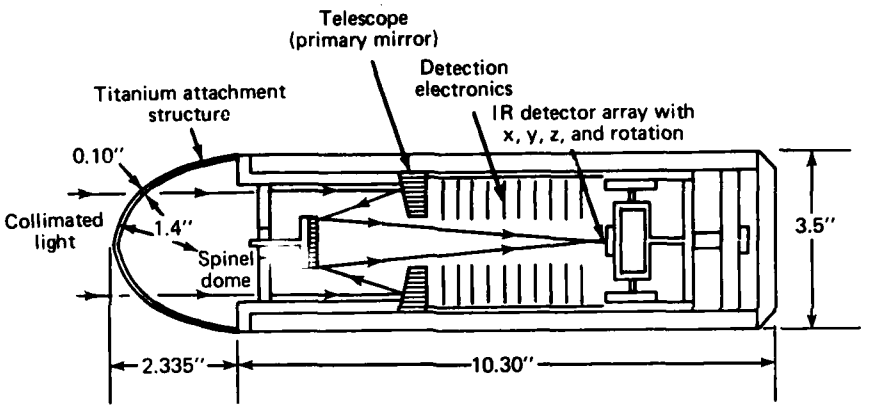


**Figure 5**—Test article in optical testing configuration.

is attached to the water-cooled holder). For calibration runs and initial dome testing, the primary instrumentation in the holder will be pressure taps, thermocouples, calorimeters, and strain gauges.

Once calibration is complete and the dome integrity is demonstrated, one of two optical systems will be inserted into the water-cooled cylindrical holder behind the dome. These are fixed-angle, *high f-number* optical systems that will be used to measure the optical characteristics of the flow. One is a reflective, Cassegrainian telescope for forward (0°) viewing, the other is a refractive, single-element telescope for off-axis viewing at 45° from the holder centerline. During initial testing, the off-axis viewing system may include a dome mounted with its centerline at an angle to the holder centerline to simulate flight angles of attack.

The test-article optics focus the IR signal radiation onto an 8-element, thermoelectrically-cooled lead selenide (PbSe) detector array with an element size of 0.004 in. and an element spacing of 0.002 in. (corresponding to 0.39 and 0.20 milliradian, respectively). The detector array is mounted on a focusable mount, allowing for precise focus adjustment, including adjustment for possible refraction of the IR signal by the nozzle expansion. During optical testing, the detector signals will be the primary output signals from the test article, augmented by thermocouples.

## 2.6 TEST INSTRUMENTATION

The test instrumentation is divided into five distinct categories. The first category is general facility instrumentation, the second is specialized facility optical instrumentation, and the final three are test-article-specific instrumentation for producing the measurements of interest.

1. Facility monitoring and control instrumentation: This instrumentation is used to control and measure the status of the facility, including temperature and pressure of the air flow, cooling water, hydrogen fuel, heater ignition, and position of the test article. These measurements will be made for all tests. In addition, special instrumentation used to survey the flow stream will be used during the facility checkout phase.
2. Instrumentation for optical signal generation and monitoring: This instrumentation produces a collimated, modulated, laser signal for optical measurements made in the facility. Special optical instrumentation will be used to measure facility-produced vibration and optical turbulence.
3. Pressure and calorimetry instrumentation: This instrumentation is to determine local flow and heat transfer on a specific test-article configuration. These measurements will be made for calibration and to support analytic predictions.
4. Thermostructural instrumentation: This instrumentation measures the temperature and stress (strain) of optical windows, window mounting (attachment), and the internal portions of the test article and its holder.
5. Optical performance instrumentation: This instrumentation is located in the test article to measure the projected IR signal or to make radiometric measurements of the infrared radiation environment.

Each type of instrumentation is discussed in the following paragraphs. Included are descriptions of the instrumentation, measurement objective, measured quantities, and signal characteristics.

### 2.6.1 Facility Monitoring and Control Instrumentation

Initial facility testing will concentrate on evaluation of the gas-handling controls, valves, cooling water flow, facility temperature-and-pressure monitoring instruments, and vitiation (hydrogen) air heater. This evaluation will use thermocouple, pressure, and flowmeter outputs that will be monitored and recorded on the PRL data acquisition system. A list of the facility control and monitoring instrumentation is given in Table 1.

Air and hydrogen flows are measured and controlled by multiple-port (12 for air, 9 for hydrogen), fast-acting digital valves. Gas pressure and temperature measurements made upstream of these valves are used in a computer algorithm to set the appropriate valve elements to achieve the desired flow. Additional pressure measurements are made in the air and hydrogen supply systems to ensure safe and proper operation. Ignition of the hydrogen-air mixture is achieved with a spark-ignited, hydrogen-oxygen ignitor. The temperature rise of cooling water through the ignitor is used to confirm the operation of this device.

All of the major facility subsystems in contact with the flow, except the test cabin shell, are water cooled. Water flow is controlled and metered using cavitating Venturi tubes at the exit of each cooling water system. Water pressure and temperature at the entrance of each Venturi tube is monitored and will be used to initiate system shutdown if specified values are not maintained. Air-flow pressures and facility wall temperatures are measured throughout the system and will monitor facility operation. A linear potentiometer will be used to measure the model injection position.

The most important measurement made during the facility checkout is the gas-flow distribution at the exit plane and downstream of the Mach 5 nozzle. These measurements will be made with probes mounted on a cross structure (rake) placed normal to the centerline of the gas stream. The rake consists of 24 total-pressure-measuring and 25 total-temperature-measuring probes, allowing a distribution of flow conditions to be determined at each downstream station. The resultant flow map will be used to determine flow conditions at various test article locations.

### 2.6.2 Optical Target Projection Instrumentation

The objective of the target projection system is to provide a readily-recognizable, target-like signal to be detected in the test article. The signal is produced by a tunable laser-diode system with multimode output power of approximately 5 milliwatts. A laser is used as a moderate-power, narrow-band source. The narrow-band nature of the signal allows easy focusing and collimation (minimize chromatic aberrations) and can provide additional discrimination by using narrow-band spectral filtering in the test article.

Laser diodes operating at a 4-$\mu$m wavelength have been selected to minimize the absorption caused by the high water content of the flow resulting from hydrogen-air combustion when the facility is operated at high total temperature. The diodes have a limited tuning capability that can be used to optimize infrared transmission (see IR transmission facility checkout experiment in Section 3.1.3). Laser radiation is collected, spatially filtered, and projected as a collimated beam into the optical window at the end of the IR signal injection assembly. The signal, therefore, appears to be a small, distant source, typical of long-range targets. Figure 3 shows the optical layout. A HeNe laser is used to adjust the optical alignment on the projection system and to index the placement of the test article at the appropriate position within the cabin for optical measurement tests. A portion (approximately 10%) of the projected IR laser beam is reflected into a focusing optic and detector system similar to that in the test article. This detection system serves as a reference for measurements made in the flow and will be used to diagnose problems such as excessive vibrations caused by the test facility.

Discrimination of the laser radiation is primarily accomplished by electronically modulating (chopping) the laser output and using the chopper frequency for detection of the IR signal, using an electronic bandpass filter. Thus very low-level signals can be discriminated against the relatively high background radiation caused by the hot flow (particularly in high pressure gas), the nozzle, and the heated test-article window. The chop frequency can be varied to maximize discrimination against unsteady (modulated) ambient radiation caused by turbulence, reflections, or contaminants in the flow. Detection capability is further enhanced by the high sensitivity of the detectors used (see description in Section 2.6.5).

The optical signal projection system is mounted on a 2 ft $\times$ 4 ft flat aluminum plate that, in turn, is rigidly attached to the granite optical table. An enclosure surrounds the projection system, providing a measure of

**Table 1**
Control and monitoring instrumentation for the
IR Seeker Aerothermal Test Facility

| Number | Function Description | Symbol | Range |
|---|---|---|---|
| 1 | Air digital input pressure | PADI | 3000 psia |
| 2 | Air digital exit pressure | PADE | 1000 psia |
| 3 | Air digital input temperature | TADI | 560° R |
| 4 | Air digital valve position | VAD01 | 0/1 |
| 5 | Air digital valve position | VAD02 | 0/1 |
| 6 | Air digital valve position | VAD03 | 0/1 |
| 7 | Air digital valve position | VAD04 | 0/1 |
| 8 | Air digital valve position | VAD05 | 0/1 |
| 9 | Air digital valve position | VAD06 | 0/1 |
| 10 | Air digital valve positon | VAD07 | 0/1 |
| 11 | Air digital valve position | VAD08 | 0/1 |
| 12 | Air digital valve position | VAD09 | 0/1 |
| 13 | Air digital valve position | VAD10 | 0/1 |
| 14 | Air digital valve position | VAD11 | 0/1 |
| 15 | Air digital valve position | VAD12 | 0/1 |
| 16 | Air-heater input pressure | PAHI | 1000 psi |
| 17 | Air-heater input temperature | TAHI01 | 2000° R |
| 18 | Air-heater input temperature | TAHI02 | 2000° R |
| 19 | Air-heater input temperature | TAHI03 | 2000° R |
| 20 | Air-heater input temperature | TAHI04 | 2000° R |
| 21 | Air-heater input temperature | TAHI05 | 2000° R |
| 22 | Air-heater exit temperature | TAHE01 | 3000° R |
| 23 | Air-heater exit temperature | TAHE02 | 3000° R |
| 24 | Air-heater exit temperature | TAHE03 | 3000° R |
| 25 | Air-heater exit temperature | TAHE04 | 3000° R |
| 26 | Heater-wall strain gauge | FHW | ? |
| 27 | Nozzle plenum pressure | PANP | 1000 psia |
| 28 | Window air-input pressure | PCAI | 2000 psia |
| 29 | Window air-output pressure | PCAO | 250 psia |
| 30 | Window air-output temperature | TCAO | 1000° R |
| 31 | Nozzle-exit static pressure | PNES1 | 15 psia |
| 32 | Nozzle-exit static pressure | PNES2 | 15 psia |
| 33 | Nozzle-exit rake pressure | PNET01 | 100 psia |
| 34 | Nozzle-exit rake pressure | PNET02 | 100 psia |
| 35 | Nozzle-exit rake pressure | PNET03 | 100 psia |
| 36 | Nozzle-exit rake pressure | PNET04 | 100 psia |
| 37 | Nozzle-exit rake pressure | PNET05 | 100 psia |
| 38 | Nozzle-exit rake pressure | PNET06 | 100 psia |
| 39 | Nozzle-exit rake pressure | PNET07 | 100 psia |
| 40 | Nozzle-exit rake pressure | PNET08 | 100 psia |
| 41 | Nozzle-exit rake pressure | PNET09 | 100 psia |
| 42 | Nozzle-exit rake pressure | PNET10 | 100 psia |
| 43 | Nozzle-exit rake pressure | PNET11 | 100 psia |
| 44 | Nozzle-exit rake pressure | PNET12 | 100 psia |
| 45 | Nozzle-exit rake pressure | PNET13 | 100 psia |
| 46 | Nozzle-exit rake pressure | PNET14 | 100 psia |

**Table 1.** (continued)

| Number | Function Description | Symbol | Range |
|---|---|---|---|
| 47 | Nozzle-exit rake pressure | PNET15 | 100 psia |
| 48 | Nozzle-exit rake pressure | PNET16 | 100 psia |
| 49 | Nozzle-exit rake pressure | PNET17 | 100 psia |
| 50 | Nozzle-exit rake pressure | PNET18 | 100 psia |
| 51 | Nozzle-exit rake pressure | PNET19 | 100 psia |
| 52 | Nozzle-exit rake pressure | PNET20 | 100 psia |
| 53 | Nozzle-exit rake pressure | PNET21 | 100 psia |
| 54 | Nozzle-exit rake pressure | PNET22 | 100 psia |
| 55 | Nozzle-exit rake pressure | PNET23 | 100 psia |
| 56 | Nozzle-exit rake pressure | PNET24 | 100 psia |
| 57 | Nozzle-exit rake temperature | TNE01 | 2300° R |
| 58 | Nozzle-exit rake temperature | TNE02 | 2300° R |
| 59 | Nozzle-exit rake temperature | TNE03 | 2300° R |
| 60 | Nozzle-exit rake temperature | TNE04 | 2300° R |
| 61 | Nozzle-exit rake temperature | TNE05 | 2300° R |
| 62 | Nozzle-exit rake temperature | TNE06 | 2300° R |
| 63 | Nozzle-exit rake temperature | TNE07 | 2300° R |
| 64 | Nozzle-exit rake temperature | TNE08 | 2300° R |
| 65 | Nozzle-exit rake temperature | TNE09 | 2300° R |
| 66 | Nozzle-exit rake temperature | TNE10 | 2300° R |
| 67 | Nozzle-exit rake temperature | TNE11 | 2300° R |
| 68 | Nozzle-exit rake temperature | TNE12 | 2300° R |
| 69 | Nozzle-exit rake temperature | TNE13 | 2300° R |
| 70 | Nozzle-exit rake temperature | TNE14 | 2300° R |
| 71 | Nozzle-exit rake temperature | TNE15 | 2300° R |
| 72 | Nozzle-exit rake temperature | TNE16 | 2300° R |
| 73 | Nozzle-exit rake temperature | TNE17 | 2300° R |
| 74 | Nozzle-exit rake temperature | TNE18 | 2300° R |
| 75 | Nozzle-exit rake temperature | TNE19 | 2300° R |
| 76 | Nozzle-exit rake temperature | TNE20 | 2300° R |
| 77 | Nozzle-exit rake temperature | TNE21 | 2300° R |
| 78 | Nozzle-exit rake temperature | TNE22 | 2300° R |
| 79 | Nozzle-exit rake temperature | TNE23 | 2300° R |
| 80 | Nozzle-exit rake temperature | TNE24 | 2300° R |
| 81 | Nozzle-exit rake temperature | TNE25 | 2300° R |
| 82 | Test-cabin pressure | PTC | 50 psia |
| 83 | Test-article location | YSI | 20 in. |
| 84 | Exhaust-differential exit pressure | PEDE | 75 psia |
| 85 | Hydrogen-supply pressure | PHS | 2500 psia |
| 86 | $H_2$ primary valve position | VHP | 0/1 |
| 87 | $H_2$ load valve position | VHLL | 0/1 |
| 88 | $H_2$ vent valve position | VHLV | 0/1 |
| 89 | $H_2$ purge valve position | VHN | 0/1 |
| 90 | $H_2$ north valve position | VH012 | 0/1 |
| 91 | $H_2$ south valve position | VH345 | 0/1 |
| 92 | $H_2$ Cell-4 fin valve | VH4F | 0/1 |
| 93 | Hydrogen digital valve pressure | PHD | 2500 psia |

**Table 1.** (continued)

| Number | Function Description | Symbol | Range |
|---|---|---|---|
| 94 | Hydrogen digital valve temperature | THD | 560° R |
| 95 | Hydrogen-line north pressure | PHLN | 1500 psia |
| 96 | Hydrogen-line south pressure | PHLS | 1500 psia |
| 97 | Heater-water pressure | PWHV | 100 psia |
| 98 | Heater-water temperature | TWHV | 660° R |
| 99 | Heater-water temperature | TWH4 | 660° R |
| 100 | Heater-water temperature | TWH7 | 660° R |
| 101 | Heater-water temperature | TWH10 | 660° R |
| 102 | Injector/mixer water pressure | PWIV01 | 100 psia |
| 103 | Injector/mixer water pressure | PWIV02 | 100 psia |
| 104 | Injector/mixer water pressure | PWIV03 | 100 psia |
| 105 | Injector/mixer water temperature | TWIV01 | 660° R |
| 106 | Injector/mixer water temperature | TWIV02 | 660° R |
| 107 | Injector/mixer water temperature | TWIV03 | 660° R |
| 108 | Injector/mixer water temperature | TWI01 | 660° R |
| 109 | Injector/mixer water temperature | TWI02 | 660° R |
| 110 | Injector/mixer water temperature | TWI03 | 660° R |
| 111 | Injector/mixer water temperature | TWI04 | 660° R |
| 112 | Injector/mixer water temperature | TWI05 | 660° R |
| 113 | Injector/mixer water temperature | TWI06 | 660° R |
| 114 | Injector/mixer water temperature | TWI07 | 660° R |
| 115 | Injector/mixer water temperature | TWI08 | 660° R |
| 116 | Signal-tube water pressure | PWSTV | 300 psia |
| 117 | Signal-tube water temperature | TWSTV | 660° R |
| 118 | Flange water pressure | PWPFV | 300 psia |
| 119 | Flange water temperature | TWPFV | 660° R |
| 120 | Nozzle-plenum water pressure | PWNPV | 300 psia |
| 121 | Nozzle-plenum water temperature | TWNPV | 660° R |
| 122 | Nozzle water pressure | PWNV | 300° R |
| 123 | Nozzle water temperature | TWNV | 660° R |
| 124 | Nozzle water temperature | TWN01 | 660° R |
| 125 | Nozzle water temperature | TWN02 | 660° R |
| 126 | Nozzle water temperature | TWN03 | 660° R |
| 127 | Nozzle water temperature | TWN04 | 660° R |
| 128 | Exhaust differential water pressure | PWEDV1 | 100 psia |
| 129 | Exhaust differential water pressure | PWEDV2 | 100 psia |
| 130 | Exhaust differential water temperature | TWEDV1 | 660° R |
| 131 | Exhaust differential water temperature | TWEDV2 | 660° R |
| 132 | Exhaust differential water temperature | TWED01 | 660° R |
| 133 | Exhaust differential water temperature | TWED04 | 660° R |

**Table 1.** (continued)

| Number | Function Description | Symbol | Range |
|---|---|---|---|
| 134 | Exhaust differential water temperature | TWED09 | 660° R |
| 135 | Exhaust differential water temperature | TWED13 | 660° R |
| 136 | Ignitor $H_2$ supply pressure | PIHS | 2500 psia |
| 137 | Ignitor $H_2$ line pressure | PIHL | 1500 psia |
| 138 | Ignitor $H_2$ marotta pressure | PIHM | 1500 psia |
| 139 | Ignitor $O_2$ supply pressure | PIOS | 2500 psia |
| 140 | Ignitor $O_2$ line pressure | PIOL | 1500 psia |
| 141 | Ignitor $O_2$ marotta pressure | PIOM | 1500 psia |
| 142 | Ignitor water pressure | PIW | 300 psia |
| 143 | Ignitor water temperature delta | TIW | 100° R |
| 144 | Ignitor $N_2$ purge pressure | PINS | 2500 psia |
| 145 | Ignitor $H_2$ primary valve | VIHP | 0/1 |
| 146 | Ignitor $H_2$ final valve | VIHF | 0/1 |
| 147 | Ignitor $O_2$ primary valve | VIOP | 0/1 |
| 148 | Ignitor $O_2$ final valve | VIOF | 0/1 |
| 149 | Ignitor $N_2$ final valve | VINF | 0/1 |

Note: Appendix A gives the nomenclature of the test-function symbols.

thermal and acoustic protection as well as protection from water leaks, dirt, and other contaminants.

Primary signals from the IR target projection system are the output of the reference detector array, the modulation reference signal, and laser system control and monitoring information. Provisions for television video are included for visual inspection, vibration, and optical turbulence measurements. Table 2 lists the signals from the IR projection system.

Future enhancements of this instrumentation can include the use of the HeNe alignment laser for measurements to be made under extremely high total temperature and pressure (i.e., water vapor) conditions, automation of the laser operation, including selection of one of four available laser diodes, and automatic operation and tuning of the laser system.

### 2.6.3 Pressure and Calorimetry Instrumentation

A hemispherical, water-cooled, combined calorimeter and pressure unit will be used to measure flow-induced, local heat-transfer flux and static pressure from calibration of the flow conditions at the test article. This unit consists of six slug calorimeters and four pressure taps mounted in a copper heat-sink body. The unit has a 1.4-in. outer radius to match accurately the geometry of the optical domes to be tested. Figure 6 shows the geometry of the unit and positions of the sensors. Maximum allowable temperature of the device is approximately 600° F.

If the unit shown in Fig. 6 is not available, separate calorimetry and pressure units will be borrowed from Acurex Corporation. Both of these devices are 2-in.-diameter hemispheres blended into 2-in.-diameter cylinders. The pressure device has 0.067-in.-diameter taps located at 0°, 7.5°, and 15° as well as on the cylinder. The calorimetry model has sensors located at 0°, 7.5°, and 15°.

Regardless of which units are used, the signals that will be reserved for these measurements are given in Table 3.

### 2.6.4 Thermostructural Instrumentation of the Infrared Window

Initial tests of the IR windows will establish their thermostructural integrity under high-speed flight conditions. No optics (see section 2.6.5) will be included in the test housing. Instead, instrumentation for monitoring the structural performance of the window and its attachment system will be used. Both ther-

**Table 2**
Target projection and test-article optical instrumentation

| Number | Function Description | Symbol | Range |
|---|---|---|---|
| A. | Target Projection Instrumentation | | |
| 150 | Target modulation frequency reference (RG 174 cable to test article and reference detectors) | SYR | 5 V |
| 151 | Reference system detector 1 | SY1 | 1 V |
| 152 | Reference system detector 2 | SY2 | 1 V |
| 153 | Reference system detector 3 | SY3 | 1 V |
| 154 | Reference system detector 4 | SY4 | 1 V |
| 155 | Reference system detector 5 | SY5 | 1 V |
| 156 | Reference system detector 6 | SY6 | 1 V |
| 157 | Reference system detector 7 | SY7 | 1 V |
| 158 | Reference system detector 8 | SY8 | 1 V |
| 159 | Reference system power indicator | SYD1 | 0/1 |
| 160 | Reference system cooling indicator | SYD2 | 0/1 |
| 161 | TV video | GY | RS 170 |
| B. | Test-Article Instrumentation | | |
| 162 | Test-article detector 1, mode A | SZ01 | 1 V |
| 163 | Test-article detector 2, mode A | SZ02 | 1 V |
| 164 | Test-article detector 3, mode A | SZ03 | 1 V |
| 165 | Test-article detector 4, mode A | SZ04 | 1 V |
| 166 | Test-article detector 5, mode A | SZ05 | 1 V |
| 167 | Test-article detector 6, mode A | SZ06 | 1 V |
| 168 | Test-article detector 7, mode A | SZ07 | 1 V |
| 169 | Test-article detector 8, mode A | SZ08 | 1 V |
| 170 | Test-article detector 1, mode B | SZ09 | 1 V |
| 171 | Test-article detector 2, mode B | SZ10 | 1 V |
| 172 | Test-article detector 3, mode B | SZ11 | 1 V |
| 173 | Test-article detector 4, mode B | SZ12 | 1 V |
| 174 | Test-article detector 5, mode B | SZ13 | 1 V |
| 175 | Test-article detector 6, mode B | SZ14 | 1 V |
| 176 | Test-article detector 7, mode B | SZ15 | 1 V |
| 177 | Test-article detector 8, mode B | SZ16 | 1 V |
| 178 | Test-article power indicator | SZ01 | 0/1 |
| 179 | Test-article cooling indicator | SZ02 | 0/1 |
| 180 | TV video | GZ | RS-170 |
| 181 | Test-article TV indicator | GZD | 0/1 |
| 182 | Test-configuration indicator 1 | JZD1 | 0/1 |
| 183 | Test-configuration indicator 2 | JZD2 | 0/1 |
| 184 | Test-configuration indicator 3 | JZD3 | 0/1 |
| 185 | Test-configuration indicator 4 | JZD4 | 0/1 |
| 186 | Reserved for dome distort. meas. | SZ1 | — |
| 187 | Reserved for dome distort. meas. | SZ2 | — |
| 188 | Reserved for dome distort. meas. | SZ3 | — |
| 189 | Reserved for dome distort. meas. | SZ4 | — |

**Table 2.** (continued)

| Number | Function Description | Symbol | Range |
|---|---|---|---|
| 190 | Telescope temperature | TZ1 | 1000° R |
| 191 | Telescope temperature | TZ2 | 1000° R |
| 192 | Telescope temperature | TZ3 | 1000° R |
| 193 | Telescope temperature | TZ4 | 1000° R |

Note: Appendix A gives the nomenclature of the test-function symbols.

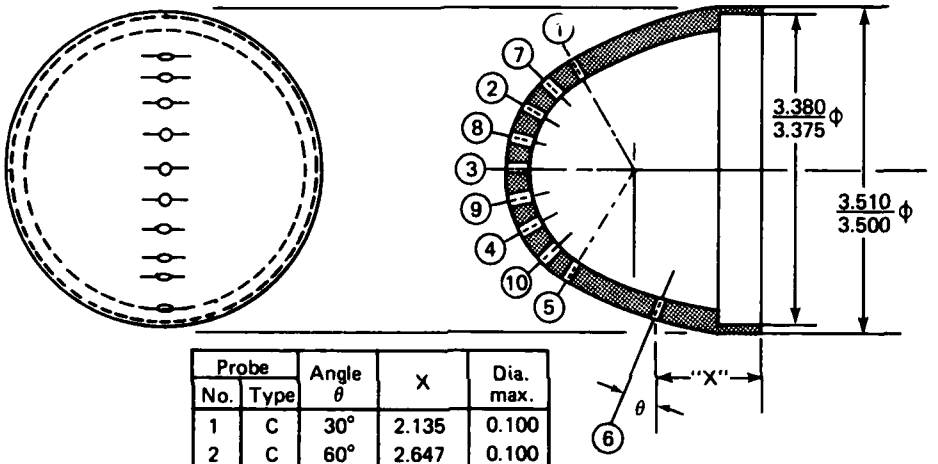


| Probe No. | Probe Type | Angle θ | X | Dia. max. |
|---|---|---|---|---|
| 1 | C | 30° | 2.135 | 0.100 |
| 2 | C | 60° | 2.647 | 0.100 |
| 3 | C | 90° | 2.836 | 0.100 |
| 4 | C | 60° | 2.647 | 0.100 |
| 5 | C | 30° | 2.135 | 0.100 |
| 6 | C | 22° | 1.120 | 0.100 |
| 7 | P | 45° | 2.425 | 0.125 |
| 8 | P | 75° | 2.787 | 0.125 |
| 9 | P | 75° | 2.787 | 0.125 |
| 10 | P | 45° | 2.425 | 0.125 |

C = calorimeter (Q = 300 Btu/ft$^2$/sec
P = pressure ($P_T$ = 100 psi)

**Figure 6**—Calibration dome for Facility pressure and calorimetry measurements.

mocouples (temperature measurement) and strain gauges (stress measurement) will be used.

Window performance will be monitored by four biaxial strain gauges mounted on the back side of the window at locations where stress are expected to be high. A chromel-alumel thermocouple will be mounted adjacent to the strain gauges to make the surface temperature measurements that are needed to convert the strain gauge measurements into stress values. Two biaxial strain gauges and four thermocouples will be installed on the uncooled metal attachment shell that acts as a transition section between the IR window and the water-cooled support structure. Table 4 lists the instrumentation signals that will be used for the thermostructural testing.

The cement used to attach strain gauges is limited to use below 1250° R. Degraded strain (stress) measurements will result if this limit is exceeded. Chromel-

alumel thermocouples are limited to operation below 2700° R. These temperatures set the allowable exposure time for the thermostructural window tests.

Small deflections of the IR window can cause significant image distortion and boresight error. Instrumentation to measure these deflections will be developed to be incorporated into the window-measuring instrumentation later. Two methods are under consideration: an amplified shadow system and an internal interferometric distance-measuring system. The latter system requires some modification of vendor hardware and a means of calibration.

**Table 3**
Pressure and calorimetry instrumentation

| Number | Function Description | Symbol | Range |
|---|---|---|---|
| 194 | Calorimeter 1 | HZ01 | 300 Btu/ft$^2$/sec |
| 195 | Calorimeter 2 | HZ02 | 300 Btu/ft$^2$/sec |
| 196 | Calorimeter 3 | HZ03 | 300 Btu/ft$^2$/sec |
| 197 | Calorimeter 4 | HZ04 | 300 Btu/ft$^2$/sec |
| 198 | Calorimeter 5 | HZ05 | 300 Btu/ft$^2$/sec |
| 199 | Calorimeter 6 | HZ06 | 300 Btu/ft$^2$/sec |
| 200 | Pressure tap 1 | PZ01 | 100 psi |
| 201 | Pressure tap 2 | PZ02 | 100 psi |
| 202 | Pressure tap 3 | PZ03 | 100 psi |
| 203 | Pressure tap 4 | PZ04 | 100 psi |

Note: Appendix A gives the nomenclature of the test-function symbols.

### 2.6.5 Optical Performance Instrumentation

The optical instrumentation consists of a collecting telescope, a detector array, a focusing mechanism, and preamplification and detection electronics. All this instrumentation is contained in a cylindrical housing that is inserted into the test-article holder atop the sting. Two types of telescopes will be used. The primary telescope is a two-mirror reflective (Cassegrainian) telescope with a 2° (total angle) field of view, a 2-in.-diameter aperture, and a 10-in. focal length. The reflective telescope is used for through-the-nozzle viewing when the axis of the test article is parallel to the flow direction or for viewing through the 45° optical port when the test article is canted at 45° to the flow. The other telescope uses a single canted germanium lens to look at angles of 0° to 45° from the axis of the test article. These refractive telescopes will be used for looking through the side 45° port and for viewing through the nozzle when the test article is canted with respect to the flow field. The field of view, aperture, and focal length of the refractive telescopes are similar to those of the reflective telescope.

Energy received by the telescope is focused on a linear detector array mounted on a translation mecha-

**Table 4**
Thermostructural instrumentation

| Number | Function Description | Symbol | Range |
|---|---|---|---|
| 204 | Thermocouple (chromel-alumel) | TZ01 | 3000° R |
| 205 | Thermocouple (chromel-alumel) | TZ02 | 3000° R |
| 206 | Thermocouple (chromel-alumel) | TZ03 | 3000° R |
| 207 | Thermocouple (chromel-alumel) | TZ04 | 3000° R |
| 208 | Thermocouple (chromel-alumel) | TZ05 | 3000° R |
| 209 | Thermocouple (chromel-alumel) | TZ06 | 3000° R |
| 210 | Thermocouple (chromel-alumel) | TZ07 | 1000° R |
| 211 | Thermocouple (chromel-alumel) | TZ08 | 1000° R |
| 212 | Thermocouple (chromel-alumel) | TZ09 | 1000° R |
| 213 | Thermocouple (chromel-alumel) | TZ10 | 1000° R |
| 214 | Strain gauge | JZ01 | $10^{-3}$ in/in |
| 215 | Strain gauge | JZ02 | $10^{-3}$ in/in |
| 216 | Strain gauge | JZ03 | $10^{-3}$ in/in |
| 217 | Strain gauge | JZ04 | $10^{-3}$ in/in |
| 218 | Strain gauge | JZ05 | $10^{-3}$ in/in |
| 219 | Strain gauge | JZ06 | $10^{-3}$ in/in |

Note: Appendix A gives the nomenclature of the test-function symbols.

nism with three linear, orthogonal degrees of freedom and independent rotation about the axis of the test article. These motions allow the array to be fine focused and the energy to be centered on the array. Rotation will allow the long dimension of the array to be oriented in an arbitrary direction relative to the flow and test article axes.

The primary sensor is an 8-element linear array of thermoelectrically-cooled PbSe detectors. The array elements have an instantaneous field of view approximately equal to the spot size formed by well-collimated light incident on an optimally-focused system. PbSe detectors were selected to provide high sensitivity (5 to $10 \times 10^9$ cm · $Hz^{1/2}$/W), middle-infrared-band coverage (3.5 to 5 $\mu$m), without the need for cryogenic cooling. A single-stage thermoelectric cooler (-20° C) requires only low voltage power for detector cooling. These detectors may also be used in the visible range although their sensitivity is lower. The array is packaged in a TO-8 can.

Detector electronics will also be housed in the telescope-detector package. Two modes of detection will be used. The primary mode is the narrow-bandpass filter mode used to detect chopped, collimated light from the IR signal injector. Output from the detector will be electronically filtered with an AC bandpass filter set to detect the signal injector modulation frequency. The modulation frequency will be high (e.g., 1 to 10 kHz) in order to discriminate against stray light. The filtered detection mode will be used to measure the blur (defocusing), image jitter, and boresight shift of the simulated target (collimated signal injector). A baseband (DC to 100 Hz) radiometric mode will also be available. This mode will sense the total radiation environment, regardless of source. Since the principal radiation sources (hot flow, dome, nozzle, etc.) are close to the telescope, the signal from these sources will be defocused and spread rather uniformly over the detector array. Separation of the effects of individual radiation sources will be determined by geometry, timing, and spectral filtering (see test descriptions, Section 3.0).

An alternate visible (silicon) array is also available and will be used if infrared measurements are precluded by excessive absorption. The visible array consists of 50 detectors in a self-scanning (multiplexed) configuration and packaged in a 16-pin dual in-line configuration. Typical integration times would be 10 to 1000 $\mu$sec. This array would only be operated in the filtered (AC) mode since visible radiometric signals are of no interest.

Signals from the output of the detector circuit (bandpass filter mode) or directly from the detectors (radiometric mode) will be amplified to a high output level (i.e., *100 mV maximum*) and digitized to ensure a high signal for collection at the recording instrumentation.

# 3.0 TEST DESCRIPTIONS

Testing during the first year of the Infrared Sensor Technology Program concentrates on proving the facility and then using it for initial experimentation with a near-term seeker concept intended for application in area-defense missiles. Facility checkout will include both operability and performance testing of the free-jet system and its instrumentation. Many of the facility measurements will be used to guide the interpretation of the initial test results and to plan future experiments. The initial set of tests serve a four-fold purpose:

1. Tests will be used to check out the design of the test article and associated instrumentation, to validate the test methods and data collection, and to determine the adequacy of the measurements for deriving the basic parameters of flow, heat transfer, and optics. Hence, the initial testing provides experience in making the necessary measurements. This experience will be used to improve the instrumentation, to refine the measurement techniques, and to determine the completeness of the data.
2. Tests will provide data that can be compared with analytic predictions. Flow, thermostructural, and optical calculations will be compared with the test results. Discrepancies will point to the need for improved theoretical understanding, more detailed models, better instrumentation and measurement techniques, and further testing requirements.
3. Tests will provide initial empirical data that cannot be readily derived analytically. Data of this type will be especially useful in advancing new seeker design concepts.
4. The tests as a whole will constitute a proof-of-principle feasibility demonstration of the initially-tested configuration (representative of a near-term area-defense missile IR seeker) and therefore can be used as the basis for an engineering or prototyping program.

This section describes the tests to be performed and includes the objective, measurement technique, and measured quantities.

## 3.1 FACILITY CHECKOUT AND CAPABILITY MEASUREMENT

This set of tests will ensure proper operation of the facility through exercising operation of the facility components, systems, and then the system as a whole. Both laboratory measurements and full system testing will be used to determine the capability of the facility to provide the necessary test conditions and to support the flow, thermostructural, and optical measurements that will be made. These measurements include determining the capability of the facility to generate the desired test conditions, the characterization of the flow (radially and axially) at the nozzle exit, and the measurement of the optical properties of the test system (including transmission and turbulence). Facility checkout will precede the test-article measurements and will continue through the initial series of flow, thermostructural, and optical testing as more instrumentation and capability are added to the system. Test-article measurement requirements and facility improvements will also dictate additional facility characterization throughout the system.

Initial facility operation will be controlled manually and therefore cannot be excessively complex. Manual system control will require a series of tests to determine the reliable, repeatable, and safe operation of the facility. After checkout of the individual facility subsystems, the facility will be operated in a series of cold (unheated) and hot (heated) flow tests that exercise the facility functions and data recording (see Table 1). Results will be used to guide facility operation during the test program. These tests will also be used for calibration and special instrumentation evaluation of facility capabilities. Ultimately the facility operation will be fully automated.

### 3.1.1. Facility Flow-Field Tests

After the air, hydrogen, cooling water, heater ignitor, and instrumentation systems have been separately checked, a series of flow-field tests will be conducted. Flow-field testing will be performed using the hydrogen combustor to heat the air. Later operation of the facility will combine the PRL stainless steel matrix heater with the hydrogen burner to reduce the water vapor resulting from hydrogen-air combustion. Flow-field uniformity is expected to improve when the matrix heater is used.

Flow-field tests will be made with air flow rates of 10 to 40 lbm/sec and hydrogen flow rates from 0.05 to 0.15 lbm/sec. Facility operating conditions are shown in Fig. 7. This figure also shows the resulting total pressure and total temperature conditions that will be evaluated in initial flow-field tests. (Figure 8 shows data for similar facility operating conditions

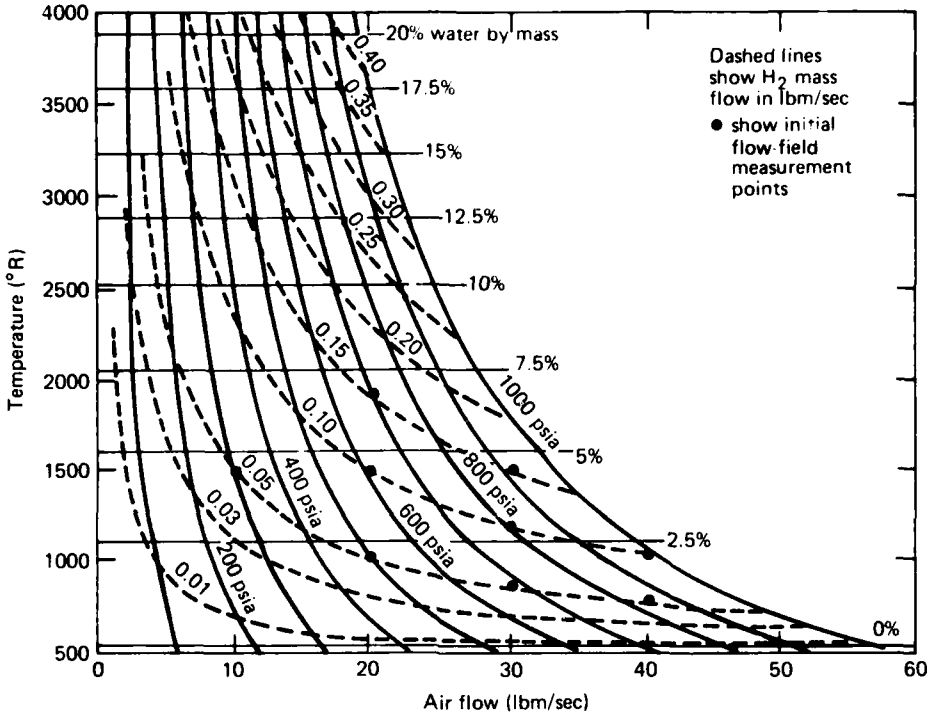


**Figure 7**—Facility operating conditions for 530°R incoming air, showing initial flow-field measurement conditions.

for the combination of the PDM heater and the hydrogen-burning heater.) Hydrogen-air mass-flow combinations that exceed 1000 psia (facility limit) or 2000° R will be excluded. This temperature limit is chosen to allow the use of chromel-alumel thermocouples and to avoid the need to water cool the rake structure. The flow field will be surveyed from the nozzle exit to 12 in. downstream, covering the region of potential IR window test locations.

In addition to defining the flow field and developing facility operating procedures, these tests will be used to evaluate the through-the-nozzle optical system. Initial testing will use an instrumented steel disk replacing the sapphire windo v of the optical signal-injector system. The disk will be instrumented to measure the temperature of the inside disk surface and adjacent gas. Gas flow rates for window cooling will be varied and the effectiveness of this window-cooling system will be evaluated. The steel disk will then be replaced with the sapphire window and a series of measurements of optical distortion will be made while looking through the flow at a resolution target located beyond the nozzle-exit position. These measurements will be made with a remotely-focussing television system (see Section 3.1.2).

Initial testing and operation of the facility will be accomplished with manual control of the system. As automated controls are developed, they will be incorporated into the test procedures. The thermal limit of the facility (4000° R) will not be approached until the facility is automated to the extent that a minimum time (< 20 sec) is spent at the extreme temperature conditions. A reliable automatic monitoring and shutdown system will also be required for operation at these conditions.

### 3.1.2 Facility Turbulence and Vibration Measurements

Turbulent mixing of air of different temperatures (densities) will produce refractive blurring and image jitter. The IR Seeker Aerothermal Test Facility can introduce cooling air upstream of the nozzle (high pressure side) to cool the window that the infrared signal enters (see Fig. 3). This cool air can also reduce the propagation path through the high-pressure, high-water-vapor gas between the window and the nozzle

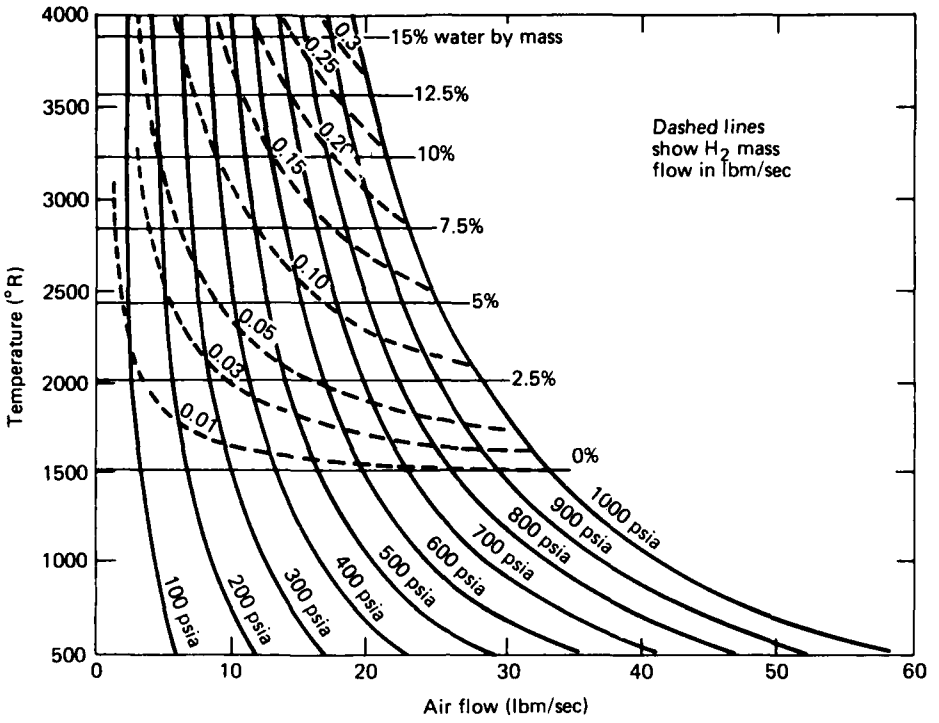


***Figure 8***—Facility operating conditions for 1500°R incoming air.

throat. Use of this capability may significantly increase turbulence in the optical path. In addition, the bend in the main air flow at the IR signal injector section and the cooling effect of the facility walls (water-cooled) may cause additional turbulence. No measurements of optical turbulence in high-pressure, high-temperature pipe flow exist. Before the facility can be used for optical measurements, an assessment of facility turbulence will be made.

Turbulence tests will be conducted using a television camera to image a resolution bar chart located in the test cabin. The camera is located on the optical table and views the same path as the IR signal projector. The test pattern will consist of a series of lines painted or inscribed on a surface located in the flow. The line width and spacing will vary from 0.1 to 0.01 in. The initial test will be made with the test surface mounted on the flow-measuring rake. If a longer measurement time is required (because of the exposure time limit of the rake), a water-cooled strut will be fabricated and marked. Television frames will be examined individually for line-pair resolution, and successive frames will be digitized and subtracted to determine short-term image movement.

Facility vibration can also induce image jitter. If the jitter frequcncy is sufficiently high, the jitter will appear as image blurring. The facility has several features intended to minimize vibration effects; these include placing the IR signal source and test article on the same 7000-lb granite block, isolating the granite block from floor vibration with air supports, partially isolating the granite block from the test cabin with flexible pressure seals, and enclosing the IR signal projection system in an acoustically isolating enclosure. Despite such precautions, some vibration effects may be observed. The television tests described above will also measure the image jitter caused by vibration. In addition, the IR signal projection system has a reference detector array that will measure vibration effects that are independent of turbulence in the flow. The combination of these measurements will be used to diagnose vibration effects.

### 3.1.3 Flow Infrared Transmission

A hydrogen burner will be used to generate high total temperatures (i.e., above 2000°R). This burner can produce a flow water-vapor concentration as high as

25% by mass. Generally the high water content is accompanied by high pressure, resulting in very high attenuation of infrared radiation. Through-the-nozzle infrared signal injection may result in very high loss since the signal must pass through the high-pressure, high-water-vapor gas upstream of the nozzle. There is a minimum in the water vapor absorption at 4 $\mu$m with an estimated transmittance of 5% over a 1-ft path (10 atm of water in 35 atm total pressure). While this transmittance is low, it is acceptable. To assess infrared transmission for through-the-nozzle signal injection, a laboratory experiment will be conducted to measure 4-$\mu$m transmission in typical facility conditions. These measurements will be used to guide the instrumentation development for optical signal injection and to determine the usable conditions for through-the-nozzle optical testing

The measurement system includes an infrared laser, a heatable, high-pressure gas cell, and a high-sensitivity IR detector. The laser radiation is modulated and detected with a lock-in amplifier. Transmission through a 1-ft path of high-pressure gas with a high water-vapor content will be measured. The high-pressure cell can be heated to 250° C, allowing a water-vapor partial pressure up to 40 atm. The cell is designed for a total pressure of at least 68 atm (1000 psi). Radiation from the laser diodes will be passed through the cell and ratioed with the signal from an evacuated cell to determine transmission. The diodes operate at several frequencies near 4 $\mu$m. The diode that optimizes the signal through the high-pressure, high-water gas (a combination of transmission and diode output) will be selected. Thus the experiment will be used to select the operating conditions of the laser diode for PRL testing. The experimental setup will also be used to make transmission measurements of infrared window materials at elevated temperatures, using a vacuum cell having a 500° C temperature capability.

### 3.2 IR SEEKER TEST CONDITIONS MATRIX

Table 5 shows the flight conditions that will be simulated during the first-years testing. Test conditions will concentrate on simulated Mach 5 flight conditions because the facility can duplicate exactly the flow and heat-transfer conditions of this flight speed. Altitudes at or below 100,000 ft will be simulated to correspond to typical tactical missile conditions.

As shown in Table 5, flight conditions at both Mach 5 and higher will be simulated. Heat transfer simulating flight conditions at Mach 5, 80,000 ft will be used for initial instrumentation checkout. Since this is the low end of the heat-transfer conditions and can be simulated without using the hydrogen burner, these conditions offer a good starting place for the initial investigations. Furthermore, Mach-5 flight speed is representative of a near-term, long-range missile and will be used for a long-thermal-soak thermostructural-window test to demonstrate the potential IR application to long-range missiles.

Higher speed flight conditions (Mach 6 and 6.5) will be used primarily to investigate the structural integrity of the IR window and attachment design under stressing high-speed flight conditions. Optical testing under these conditions will be directed toward measuring dome (and flow) radiation under high-temperature conditions and toward determining the effects of high thermal gradients in the window on optical distortion.

Table 5 also gives a description of the facility conditions in terms of total temperature and pressure, mass-flow rate, cold-wall heat flux, air heater used, and resulting water concentration (i.e., hydrogen burner output) in the flow. These quantities are fundamental measures of the flight conditions.

Tests will proceed from least stressing conditions to most, and from flow and calorimeter tests to thermostructural tests (with and without instrumentation on the dome), and then to optical tests. A brief description of the purpose of each type of test is given in the table. It is anticipated that a number of tests will be repeated as instrumentation and experimental techniques might improve, as new designs are tested, and as a check of the repeatablility of results.

The initial series of tests (1 through 17) will simulate flight at 0° angle of attack and 0° look angle (sensor looking directly forward). The second series (18 through 27) simulate an unsymmetrical optical case with the IR dome and seeker look angle at 45° to the flow axis. The unsymmetrical flow and unsymmetrical heating conditions of the second series are expected to lead to optical boresight errors and different thermostructural conditions.

Pressure and calorimetry tests will be limited to 5 sec. The duration of other tests will be 15 to 20 sec. However, long-duration (i.e., 10-minute) thermostructural tests may be conducted at the end of the scheduled tests if a spare dome is available and good results are anticipated from the analytical predictions and experience gained from previous tests. This long-duration experiment will be conducted at simulated Mach 5, 80,000 ft conditions.

Conduct of each individual test will be made in accordance with a test sequence that documents:

1. Test condition.
2. Test article.

**Table 5.**
Test matrix for the IR Seeker Aerothermal Facility

| Flight Condition | | | IR Seeker Aerothermal Test Facility Condition | | | | | | |
|---|---|---|---|---|---|---|---|---|---|
| Test No. | Mach No. | Altitude (ft × 1000) | Total Temp. (°R) | Total Pres. (psia) | Mass Flow (lbm/sec) | Heater* | Mass $H_2O$ (%) | Heat Transfer (Btu/ft$^2$/sec) | Test Purpose |
| Tests with model in forward position (dome axis parallel to flow axis) | | | | | | | | | |
| 1 | 5.0 | 80 | 2000 | 230 | 7 | PDM | 0 | 51 | Flow measurement (pressure and calorimetry) |
| 2 | 5.0 | 80 | 2000 | 230 | 7 | $H_2$ | 7 | 51 | |
| 3 | 6.5 | 100 | 3500 | 540 | 12 | PDM + $H_2$ | 12 | 75 | |
| 4 | 6.0 | 80 | 2900 | 780 | 18 | PDM + $H_2$ | 8 | 90 | |
| 5 | 5.0 | 50 | 2000 | 960 | 27 | PDM | 0 | 101 | |
| 6 | 5.0 | 50 | 2000 | 960 | 27 | $H_2$ | 7 | 101 | |
| 7 | 5.0 | 80 | 2000 | 230 | 7 | PDM | 0 | 51 | Dome temperature and radiance (thermocouples and radiometer) |
| 8 | 5.0 | 80 | 2000 | 230 | 7 | $H_2$ | 7 | 51 | |
| 9 | 6.5 | 100 | 3500 | 540 | 12 | PDM + $H_2$ | 12 | 75 | |
| 10 | 6.0 | 80 | 2900 | 780 | 18 | PDM + $H_2$ | 8 | 90 | |
| 11 | 5.0 | 50 | 2000 | 960 | 27 | PDM | 0 | 101 | Thermal shock (thermocouples and strain gauges) |
| 12 | 5.0 | 50 | 2000 | 960 | 27 | $H_2$ | 7 | 101 | |
| 13 | 5.0 | 80 | 2000 | 230 | 7 | PDM | 0 | 51 | Optic measurement (image spread and jitter radiance) |
| 14 | 5.0 | 80 | 2000 | 230 | 7 | $H_2$ | 7 | 51 | |
| 15 | 6.5 | 100 | 3500 | 540 | 12 | PDM + $H_2$ | 12 | 75 | |
| 16 | 6.0 | 80 | 2900 | 780 | 18 | PDM + $H_2$ | 8 | 90 | |
| 17 | 5.0 | 50 | 2000 | 960 | 27 | PDM | 0 | 101 | " " |
| Tests with model in aft position (dome axis 45 degrees from flow axis) | | | | | | | | | |
| 18 | 5.0 | 80 | 2000 | 230 | 7 | PDM | 0 | 51 | Flow measurement (pressure and calorimetry) |
| 19 | 5.0 | 80 | 2000 | 230 | 7 | $H_2$ | 7 | 51 | |
| 20 | 6.5 | 100 | 3500 | 540 | 12 | PDM + $H_2$ | 12 | 75 | |
| 21 | 6.0 | 80 | 2900 | 780 | 18 | PDM + $H_2$ | 8 | 90 | " " |
| 22 | 5.0 | 50 | 2000 | 960 | 27 | PDM | 0 | 101 | " " |
| 23 | 5.0 | 80 | 2000 | 230 | 7 | PDM | 0 | 51 | Optical measurement (image spread and jitter, radiance, and boresight error) |
| 24 | 5.0 | 80 | 2000 | 230 | 7 | $H_2$ | 7 | 51 | |
| 25 | 6.5 | 100 | 3500 | 540 | 12 | PDM + $H_2$ | 12 | 75 | |
| 26 | 6.0 | 80 | 2900 | 780 | 18 | PDM + $H_2$ | 8 | 90 | |
| 27 | 5.0 | 50 | 2000 | 960 | 27 | PDM | 0 | 101 | |

*$H_2$ ≡ hydrogen heater; PDM ≡ Pittsburgh-Des Moines storage heater.

3. Facility operation.
4. Measurements to be made.
5. Data recording and reduction plan.

Further information on the measurements to be made and the data recording and reduction is given in Sections 3.3 through 3.5.

## 3.3 TEST-ARTICLE MEASUREMENTS

Three basic kinds of measurements will be made in the facility. First, each of the test conditions of Table 5 will be measured with pressure and calorimetry instrumentation to confirm the flow conditions and heat-transfer predictions. Second, an instrumented IR dome (window) with thermocouple and strain gauge instrumentation will be used to demonstrate dome survival and attachment design, while temperature and strain data are collected to be compared to analytic predictions. Finally, optical measurements will be made with a telescope and IR detector array behind the dome. These optical measurements will collect boresight shift, image blur, and radiometric data from the combined effects of flow and dome heating and distortion.

### 3.3.1. Pressure and Calorimetry Measurements

Pressure and calorimetry measurements are made to ensure accurate knowledge of the flow conditions produced by the facility. In particular, these measurements will confirm that the presence of the model does not significantly influence the flow conditions as measured by the rake system (see Section 3.1.1).

A water-cooled hemispherical pressure and calorimetry unit will be used to make measurements of static pressure and local heat transfer at several locations around the dome. An analysis of transient heat transfer has shown that the uncooled unit can be held in the stream for 3 sec before the temperature of the copper body exceeds 1160° R. This is sufficient time to make the measurements. The water-cooled option will allow measurement times to be greater than 5 sec. under all facility operating conditions.

As shown in the test matrix of Table 5, the first six tests will be used for pressure and calorimetry measurements. The tests were selected to obtain data sequentially from the lowest to the highest heat-flux cases, allowing measurement experience to be successively applied to more severe test conditions. A second series of pressure and calorimetry tests (tests 18 through 22) will be conducted with the test article located in a downstream position. These measurements will be made to support optical measurements to be made at a 45° angle to the flow centerline (using the upper 45° window in the test cabin). Data taken in this series of tests will be compared to analytical predictions of pressure and heat transfer around a hemispherical dome, using the rake measurements to define the flow field.

### 3.3.2. Window Thermostructural Measurements.

Thermostructural tests of the IR window and the uncooled attachment structure will be made before optical testing. Four hemispherical spinel domes will be available for testing. These domes will be mounted on a titanium or columbium (niobium) attachment structure that holds the dome and forms a transition structure between the dome and the water-cooled jacket of the test-article holder. The thermocouples and strain gauges will both be mounted on the spinel domes and attachment structure.

Tests 7 through 10 of Table 5 will be conducted with a spinel dome instrumented with thermocouples. The primary purpose of these tests is to establish the reliablilty of the dome and its attachment. The test time will be carefully controlled to ensure that the metal attachment section does not exceed temperature limits (about 1500° R for titanium, much higher for columbium). Tests will proceed from low to high heat transfer conditions and the dome assembly will be inspected after each test. The thermocouple data will be reviewed to discover deviations from predictions.

Tests 11 and 12 will be conducted to determine the thermal shock survival of the dome assembly under high heat-flux conditions. These tests will use a dome instrumented with two biaxial strain gauges and two thermocouples with an attachment structure instrumented with a single strain gauge and thermocouple. Test time will be limited on the basis of the temperature limitations of the test assembly.

The thermal radiation for the dome and its effect on the seeker is an important aspect of the IR-dome design. During the thermostructural test series, measurements will be made of the total radiant flux from the inner surface of the dome. A low-flux calorimeter will be installed behind the dome and used to measure the time history of radiant heat transfer. These data will be used to make an estimate of dome radiation. Since there will be significant time-independent radiation from the gas flow, the time-dependent portion of the radiant transfer will be used to determine the radiation from the dome as it heats.

At the conclusion of the thermostructural tests (7 through 12), adequate data will be available to certify the dome and attachment for continuation into the optical tests. The temperature and strain data will be compared to predictions made with heat-transfer and

thermal-stress codes to assess the accuracy of the predictions. If substantial differences are found, the tests will be repeated to determine the variablility of the test results.

### 3.3.3. Optical Measurements

Optical measurements will be made to determine the optical effects of high-speed flight on the achievable sensor resolution, sensitivity, and accuracy of angle measurement. In turn, these measurements will be used to make assessments of the performance of the seeker configuration under a variety of operational conditions and will form a data base for design of missile seekers.

Three basic types of optical measurements will be made. These are image blur, image boresight shift, and background flux. Table 6 lists these measurements and their effects on seeker performance. Blur and boresight measurements will be made using a collimated infrared source projected into the test article. The source will be modulated at high frequency (e.g., 1 kHz) and detected with a narrowband amplifier circuit that uses the laser modulator signal as a reference. Background flux measurements will be made radiometrically, i.e., no signal is present and the low frequency (DC to approximately 100 Hz) output of the detector will be amplified and recorded. All three measurements can be made simultaneously, but, typically, radiometric mea-

**Table 6**
Parameters for evaluation of the optical performance of High-Speed IR Seekers

| Parameters | Effect of Guidance | Measurements |
|---|---|---|
| Flow field (from nozzle) | Determines flow conditions around the IR window. | Flow velocity, temperature, pressure, and water content. |
| Flow field (around window) | Determines optical effects of flow (shock refraction, density gradients, turbulence), and flow radiation. Determines heat transfer to the IR window and attachment structure. | Flow pressure and heat-transfer rate; total radiative heat transfer. |
| Heat transfer (to the window) | Determines window heating, window distortion, and material deterioration. Temperature distribution determines thermal stresses. | Window temperature; total radiative heat transfer (heating of optics, gimbal, stabilization, etc.). |
| Thermal stress | Determines window survival, attachment design, and window distortion (reaction to thermal expansion). | Strain (window and attachment). |
| Optical | (Determined by the above effects.) | |
| – image blur | Determines available target signal and angular discrimination capability (e.g., clutter suppression and target. separation). | Point-source image profile at focal point (point spread function). |
| – image movement | Determines system response and noise (tradeoff between movement and blur). | Time history of the point-spread function. |
| – boresight error | Coupling of body motion into guidance. Tracking noise. | Image center on focal plane. |
| – optical radiation | Determines system sensitivity, dynamic range, and potential false targets (scan modulation of stray radiation). | Radiance on the focal plane (all sources: facility, flow, dome). |

surements will be made only for short times during a typical test run. Each kind of measurement is discussed below in detail.

Before the start of a test run, the optical characteristics of the test article (mounted in the string) will be measured by projecting a chopped, collimated beam into the telescope while the test article is in the test position in the test cabin. The test-beam image on the focal plane of the detector will be measured to determine the size of the image (typically a single detector will encompass the 90% containment circle) and the location on the image plane. These measurements will be references for the blur and boresight error test measurements to be made in the flow field. After the optical measurements for reference are made, the test article will be retracted into the test cabin, and a baseline radiometric measurement will be made to determine the ambient flux level in the test cabin.

The facility flow will be started with the test article in the stowed position. Once steady flow has been achieved in the cabin, the protective shield is raised and the model is rapidly inserted into the flow. Radiometric measurements are made as the model is inserted to determine the radiation from the flow. (Note that this measurement is not typical of flight-condition radiation since the flow has a very high water content. Furthermore, the nozzle and upstream gases and other facility components are expected to contribute heavily to radiation in the test chamber.) As the infrared window (dome) on the test article heats, the change in window temperature results in an increase in the radiometric signal seen by the detectors. At the end of a test run either (1) the flow will be shut off, and radiometric measurements made without the flow present or (2) the test article will be quickly withdrawn from the flow and radiometric measurements will be made in the ambient environment of the test cabin. Either method will allow an approximate estimate to be made of the high-temperature window (dome) radiation. Ambient test-cabin or test-area radiation will serve as a reference for dome radiation measurements made after heating and without flow. If method 1 is used, the decrease in DC radiation with time after facility shutdown is an indicator of the residual radiation of the nozzle and other water-cooled parts of the test facility. It is expected that cooling of the test-article window will be much slower than that of the water-cooled facility components.

Boresight and blur measurements are made by noting the distribution of the projected target image on the IR-detector array. Typically, the target signal will be measured with an integration time of 10 msec resulting in image data with a 100-Hz bandwidth. Data recording at this bandwidth will allow post-test analysis to determine the presence of low frequency jitter in the image location. Image blur is measured by determining the amount of signal on the individual detector elements and using the distribution to estimate the 90% energy-containment region (as an estimate of the usable sensor resolution). Boresight shifts are determined from either the peak or the centroid of the energy distribution (both measures will be used). Reference detectors in the signal projection system monitor the projected signal and will be used to determine potential corrupting factors, such as jitter of the signal beam, caused by facility vibration.

Both test-article and reference signals will be recorded digitally for further data reduction and for comparison to analytical results. These data are primarily the optical measurements that will be used to determine the optical performance of the seeker under high-speed flight conditions.

Two series of optical tests will be made. The first measures the optical parameters for the geometrical case where the optical axis and the centerline of the flow-field coincide. The symmetry of this geometry gives no boresight error, only image spread and jitter. Symmetrical geometry optical parameters, including in-band radiance, are measured in tests 13 through 17 (see Table 5). The second series simulates a nonsymmetrical optical geometry. The IR dome will be mounted at an angle 45° to the axis of the test-article holder (and to the flow field centerline). The optical telescope will look toward the 45° window on the test cabin and the IR signal will be injected into this window. In tests 23 through 27, the flow field and heating of the dome is off the optical centerline causing optical boresight errors. Unsymmetric blurring is also expected. This test condition will also be less subject to radiation from the upstream flow in the nozzle throat and from signal attenuation caused by water vapor.

## 3.4 DATA RECORDING AND FACILITY CONTROL

The Data Acquisition subsystem (DAS) of the PRL Digital Data Acquisition And Control System (DIDACS) will be used for recording facility and test-article data. DIDACS is a hierarchical supervisory control system that contains subsystems to control the facility and operational sequences of the test-article, including scheduling setpoint conditions of the various control loops in the analog control subsystem and direct digital control of air-mass flow and temperature. The supervisor also controls operation of the

DAS, providing various sampling rates and sequences, turning recording on and off, and synchronizing data that is preprogrammed as part of the sequence of the test operation.

DAS capability is wired into the IR Seeker Aerothermal Test Facility (Cell 4 of PRL). DAS provides data recording for up to 50 channels of midband multiplexed data and up to 576 channels of DC data, using submultiplexers. Four channels of wide-band data recording are available, each capable of a 10-kHz sampling rate. Specifications for these data-recording subsystems are shown in Table 7.

Control of the facility tests will be accomplished using the upgraded DIDACS shown in Fig. 9. Facility operation will be controlled by the supervisor process resident in an Eclipse computer (Data General) via the state-control, direct-digital-control, and analog-control subsystems. The test supervisory control sequence is designed by the test engineer to provide automatic operation of the test article and can contain iterative and branched alternative sequences to provide rapid, error-free progression through the test. This capability also provides for safe facility shutdown or alternative test sequences based on the real-time determination of test progress from test data, facility monitoring, or manual intervention.

The state-control subsystem provides output and monitoring of all binary (on/off) final control elements and indicators. The subsystem has 100 binary output channels and an equal number of inputs. In operation, the state-control subsystem outputs digital words to provide control states defined by the test sequence and monitors the status of all binary states. Monitored information is reported to the supervisor for appropriate response. The state-control subsystem is implemented in a Nova computer (Data General) using a DG/DAC interface unit.

The direct-digital-control subsystem is used to control facility air-mass flow and temperature. In the IR Seeker Aerothermal Test Facility, mass flow is controlled by two digital control valves, and a third digital valve provides temperature control by adjusting the hydrogen-mass flow to the vitiation air heater. In later testing, the ratio of the output from the two air-flow valves will control the temperature of the process air at the output of the storage heater.

The analog-control subsystem is a computer-based unit that provides control of up to eight parameters,

**Table 7**
Data-acquisition capabilities of PRL

| Data Recorder | Number of Channels | Bandwidth (Hz) | Signal Level | Full-Scale Accuracy | Comments |
|---|---|---|---|---|---|
| Digital data recorder | 384 | DC – 1 | 5-100 mV | ±1% | Pressure submultiplexer |
| | 192 | DC – 1 | 5-100 mV | ±0.5% | Temperature submultiplexer |
| | 20 | DC – 1 | 0-100 kHz | ±0.25% | Freq. output transducers |
| | 50 | DC – 400 | 5-100 mV | ±0.25% | Mid-band multiplexer |
| | 4 | DC – 4000 | 5 V | ±0.25% | Wide-band multiplexer |
| Oscillo-graph | 12 analog | DC – 3000 | 1-500 mV/div | ±1% | Fiber optics CRT oscillograph recoder |
| Strip-chart recorder | 12 analog | DC – 1 | 50-500 mV/div<br>0-1 mV<br>0-2 mV<br>0-5 mV<br>0-10 mV<br>0-20 mV<br>0-50 mV<br>0-100 mV<br>0-200 mV<br>0-500 mV<br>0-1 V | ±0.5% | Any channel can also be used with frequency output transducers |

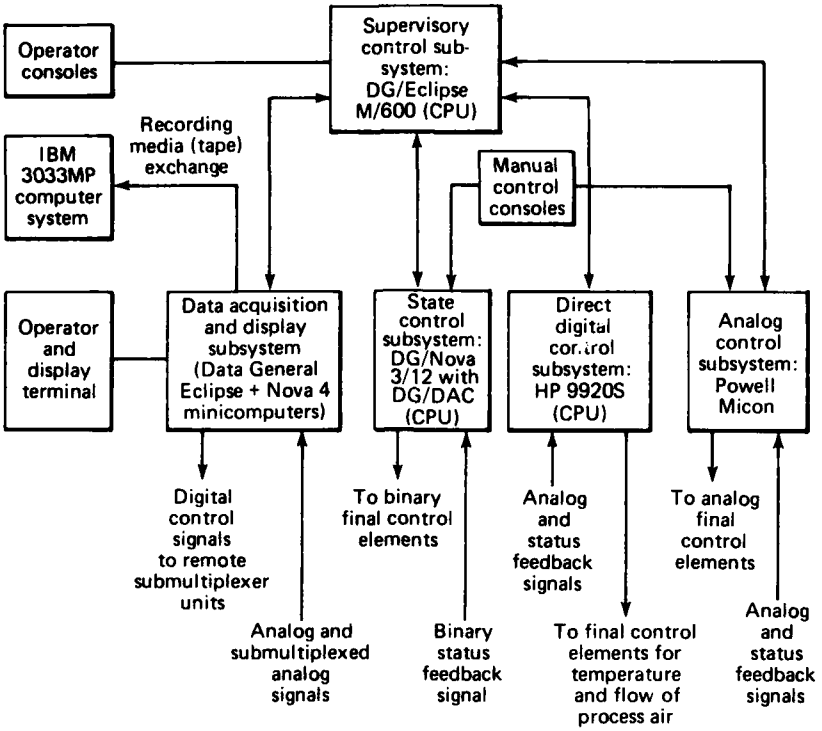


**Figure 9**—PRL instrumentation and control system for automated testing in the IR Seeker Aerothermal Test Facility.

using closed-loop feedback. A wide range of transfer-function algorithms can be programmed, and control constants can be easily changed. Setpoints for each loop are provided by the supervisor and are updated as required throughout the control sequence. Loop status is returned to the supervisor and may be used for monitoring as required.

Appendix B gives a summary of a typical test sequence. The functions described in this sequence will be controlled by DIDACS.

## 3.5 DATA REDUCTION AND REPORTING

All data produced by the facility and test instrumentation will be available for both real-time display and immediate playback for a quick-look assessment of the data quality. After each check-out run or test, the data will be compared to the expected results to determine the proper functioning of the facility and data recording and to indicate the success of the measurement.

Before a test is run, analytical results will be available for comparison to the test results. Comparison between analytical and test results will be made immediately after each test. If there is significant deviation between analysis and test, a check will be made of the facility operating conditions and diagnostic measurements to determine whether a valid test was run. If no error can be found, the test may then be repeated to determine the reproducability of the data on a run-to-run basis.

Pressure and calorimetry measurements will be compared to flow calculations made using the facility flow-field profiles measured with the instrumented rake. If the test article blockage does not significantly alter the nozzle performance (as is expected from original nozzle characterization data), the flow predictions will agree with the measured pressure and heat-transfer data.

IR window temperature and strain (stress) measurements made during thermostructural testing will be compared to predictions from a finite-difference heat-transfer calculation (using the APL URLIM code) combined with a finite-element stress code (SAAS III or NASTRAN). Initial temperature and stress predictions will be made using rake-measured flow conditions and will be updated on the basis of pressure and calorimetry measurements, if needed. Temperature

predictions, combined with the spectral emissivity of the window from laboratory measurements, will be used to estimate total radiant flux from the dome into the radiometric sensor. These estimates will be compared to total radiant-flux measurements made during the thermostructural tests. Actual test temperature data, if deviating significantly from predictions, will be used to recalculate the total radiant flux inside the dome.

Optical measurements of the performance of the IR window will be compared to analytic predictions of image defocussing and boresight error. These predictions will be made on the basis of flow conditions and heat transfer resulting in dome distortion. Banded (spectral) radiometric measurements will be compared to estimates on the basis of dome temperature measurements (see above).

After optical measurements are made, the data will be reduced to make more accurate estimates of the optical parameters. Outputs from all eight detectors will be processed to determine energy centroid, energy peak, and spot size. Integration of successive data frames may be used to decrease noise effects and to determine more accurately the trends in blurring and boresight error. Spectral analysis of the time history of the energy peak (or centroid) will be used to determine low-frequency image jitter (to 100 Hz bandwidth).

Raw data experiments in engineering units will be graphed and distributed in a raw-data-book form immediately following each test (next day). The data book will contain a brief description of the test, the test plan sheets, facility operation log, and time-history data. Recorded data (including video tapes) will also be available immediately after each test.

## 4.0 TEST SCHEDULE

The testing schedule is given in Table 8. The first part of 1985 is devoted to construction of the test facility and the associated instrumentation. Following completion of the facility, a series of tests will be performed to confirm the proper facility operation and control and to measure the facility and instrumentation performance. These tests will be made to verify the proper functioning of the primary measurement instrumentation and to uncover effects that may seriously affect measurement capabilities.

Actual testing of the IR seeker will commence in late July with a series of flow and calorimetry measurements designed to determine actual test conditions and to provide data for window heating, thermal stress, and optical analysis. Repeatability of test condtion will also be determined. After the test conditions are measured, a series of tests of window thermostructure will be conducted to determine the ability of the IR window to survive the high heating environments. These tests will also validate the window attachment design in a realistic-flight thermal environment. The thermostructural testing will use a highly-instrumentated window that is unsuitable for optical measurements. The initial series of measurements will conclude with an optical performance evaluation made with the same flight conditions as were used for the measurements of flow and thermostructure.

Four major testing reports will be written:

1. Test Plan (this document, TG 1349),
2. Facility Description and Performance Report,
3. Test Article and Instrumentation Report, and
4. Test Results and Conclusions.

These four reports will completely document the test program for the 1985 IRAD Infrared Sensor Technology Program. The schedule for report completion is given in Table 8.

**Table 8**

**1985 test schedule for IR Seeker**

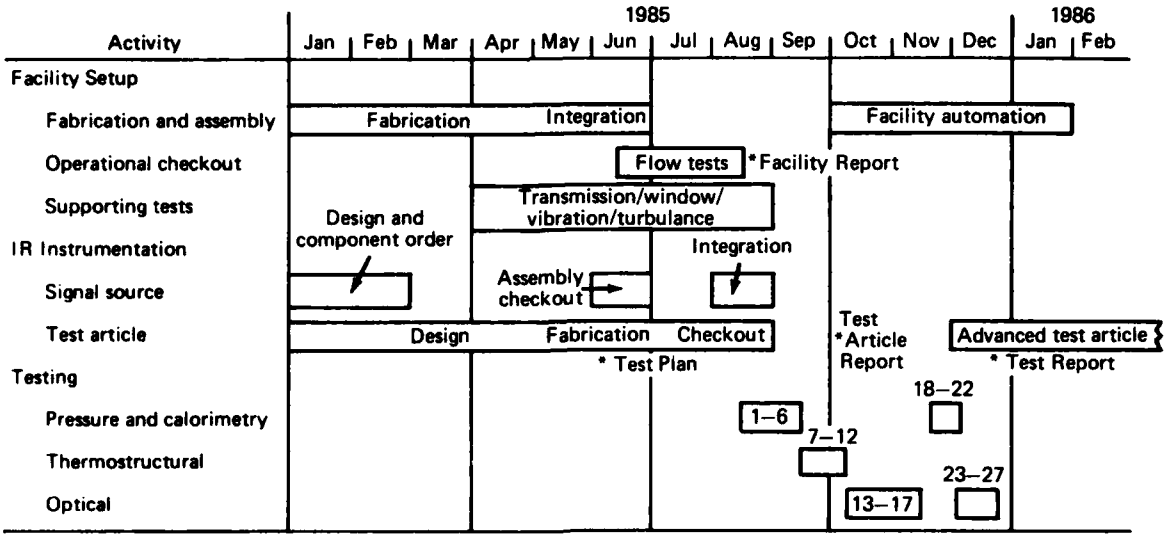

# APPENDIX A
# TEST FUNCTION SYMBOL NOMENCLATURE

Following are the symbol definitions used to denote measured quantities listed in Tables 1 through 4.

| Symbol | First Position | Other Positions |
|---|---|---|
| A | Area (sq.in.) | Air |
| B | | Bypass |
| C | Time (sec) | Combustor/cooling/ cabin |
| D | | Diffuser/digital |
| E | Voltage (V) | Exit/exhaust |
| F | Force (lbf) | Fuel/final |
| G | Video (TV) | |
| H | Heat (Btu/ft$^2$/sec) | Hydrogen/heater |
| I | Current (A) | Inlet/ignitor/injector |
| J | Strain (in/in) | Ramjet |
| K | | |
| L | Length (in) | Line/load |
| M | Mach number | Mix/marotta |
| N | | Nitrogen/nozzle |
| O | | Oxygen/open/on |
| P | Pressure (psia) | Position/primary/ plenum |
| Q | Flow (gpm) | |
| R | Radial location (deg) | Rocket/regulator/ reference |
| S | Signal | Static/supply/seeker |
| T | Temperature (°R) | Total/tank/test |
| U | Velocity (ft/sec) | |
| V | Valve ID | Vent/vitiation |
| W | Mass flow (lbm/sec) | Water/wall window |
| X | Axial location (in) | Closed/off |
| Y | Radial location (in) | Optical reference |
| Z | Altitude (ft × 1000) | Model (test article) |

# APPENDIX B
# TYPICAL TEST SEQUENCE

Following is a typical operating sequence for testing in the IR Seeker Aerothermal Test Facility. Test-specific information, such as the different test conditions, test articles, and measured quantities are not included. Measured quantities are given in Tables 1 through 4.

1. Data system turned on; low-speed operation.
2. Instrumentation checkout sequence and optical table balancing.
3. Steam ejector on (if needed).
4. Cooling water on.
5. Air flow on; low rate (< 5 lb/sec).
6. Heater ignitor on.
7. Data system to high-speed operation.
8. Hydrogen flow on; low rate.
9. Air and hydrogen flow ramped to test condition.
10. Ignitor off.
11. Lift shield; insert test article into flow.
12. Conduct the test.
13. Remove the test article from the flow; drop the shield.
14. Set data system to low rate.
15. Hydrogen and air flow ramped down; hydrogen to off, air to low rate.
16. Air flow shut off after one minute.
17. Steam ejector off.
18. Cooling water off.
19. Data system off.

# INITIAL DISTRIBUTION EXTERNAL TO THE APPLIED PHYSICS LABORATORY*

The work reported in TG 1349 was done under Navy Contract N00024-85-C-5301. This work is related to Task X8G5, which is supported by The Johns Hopkins University Applied Physics Laboratory Independent Research and Development Program.

| ORGANIZATION | LOCATION | ATTENTION | No. of Copies |
|---|---|---|---|
| DEPARTMENT OF DEFENSE | | | |
| Secretary of Defense | Washington, DC 20301 | G. C. Kopesak, OUSDRE (ET) | 1 |
| Defense Technical Information Center | Alexandria, VA 22314 | Accessions | 12 |
| DEPARTMENT OF THE NAVY | | | |
| CNO | Washington, DC 20350 | OP 98 | 1 |
| | | OP 983 | 1 |
| | | OP 987 | 1 |
| | | OP 987B | 2 |
| | | OP 35 | 1 |
| | | OP 35E | 1 |
| | | OP 352L | 1 |
| | | OP 355W | 1 |
| | | OP 507D | 1 |
| Office of the Assistant Secretary of the Navy (RE&S) | Washington, DC 20350 | Edward Donalson | 1 |
| | | Charles Kincaid | 1 |
| | | R. E. Metry | 1 |
| | | R. L. Rumpf | 1 |
| NAVSEASYSCOM | Washington, DC 22202 | SEA 06 | 1 |
| | | SEA 06A | 1 |
| | | SEA 06AT | 1 |
| | | SEA 06AX | 1 |
| | | SEA 06P | 1 |
| | | SEA 06R | 1 |
| | | SEA 62 | 1 |
| | | SEA 62B | 1 |
| | | SEA 62R | 2 |
| | | SEA 62R1 | 2 |
| | | SEA 62R11 | 1 |
| | | SEA 62R2 | 1 |
| | | SEA 62R4 | 1 |
| | | SEA 62R5 | 2 |
| | | SEA 62R52 | 1 |
| | | SEA 62Z | 1 |
| | | SEA 62Z1 | 1 |
| | | SEA 62Z2 | 1 |
| | | SEA 62Z3 | 1 |
| | | SEA 62Z3B | 1 |
| | | SEA 62Z31 | 2 |
| | | SEA 62Z31F | 1 |
| | | Library, SEA 9961 | 2 |
| | | PMS 400 | 1 |
| | | PMS 400B | 1 |
| NAVAIRSYSCOM | Washington, DC 22202 | AIR 320 | 1 |
| | | AIR 320B | 1 |
| | | AIR 320D | 1 |
| | | AIR 320R | 1 |
| | | AIR 06 | 1 |
| | | AIR 0623 | 1 |
| | | Library, AIR 7226 | 2 |
| NAVPRO | Laurel, MD 20707 | | 1 |

**Requests for copies of this report from DoD activities and contractors should be directed to DTIC. Cameron Station, Alexandria, Virginia 22314 using DTIC Form 1 and, if necessary, DTIC Form 55.**

*Initial distribution of this document within the Applied Physics Laboratory has been made in accordance with a list on file in the APL Technical Publications Group.

# INITIAL DISTRIBUTION EXTERNAL TO THE APPLIED PHYSICS LABORATORY

| ORGANIZATION | LOCATION | ATTENTION | No. of Copies |
|---|---|---|---|
| Naval Surface Weapons Center | Dahlgren, VA 22448 | NSWC/DL D2W | 1 |
| | | NSWC/DL G21 | 1 |
| | | NSWC/DL G22 | 1 |
| | | NSWC/DL G24 | 1 |
| | | Library | 2 |
| | White Oak, MD 20903-5000 | NSWC/WO G40 | 1 |
| | | NSWC/WO K22 | 1 |
| | | NSWC/WO N12 | 1 |
| | | Library | 2 |
| Naval Weapons Center | China Lake, CA 93555-6001 | 3906 | 2 |
| | | 3921 | 1 |
| | | 3942 | 1 |
| | | Library | 1 |
| Office of Naval Technology | Arlington, VA 22209 | ONT 07C | 1 |
| | | ONT 0712 | 1 |
| | | ONT 0713 | 1 |
| Pacific Missile Test Center | Pt. Mugu, CA 93042 | 4045 | 1 |
| U.S. Naval Academy | Annapolis, MD 21402 | Dir. Research | 2 |
| DEPARTMENT OF THE ARMY | | | |
| Missile Command | Redstone Arsenal, Huntsville, AL 35898 | DRSMI OD | 1 |
| | | DRSMI RR | 1 |
| Ballistic Missile Defense Advanced Technology Center | Hunstville AL 35807 | ATC-R | 1 |
| | | Price Boyd, ATC-RN | 1 |
| | | HNV | 1 |
| | | LEH | 1 |
| DEPARTMENT OF THE AIR FORCE | | | |
| Air Force Armament Div. | Eglin AFB, FL 32542 | AD/XRG | 1 |
| Aeronautical Systems Div. | Wright-Patterson AFB, Dayton, OH 45433 | YYM | 1 |
| CONTRACTORS | | | |
| Acurex Corporation | Huntsville, AL 35806 | F. Strobel | 1 |
| Coors Porcelain Co. | Golden, CO 80401 | D. Roy | 1 |
| General Dynamics | Pomona, CA 91766 | H. J. Meltzer | 2 |
| | | R. M. Pietrasz | 1 |
| | | R. Parker | 1 |
| | | J. Stamper | 1 |
| Hughes Aircraft Co. | Canoga Park, CA 91304 | R. R. Miller | 2 |
| | | A. V. Funari | 1 |
| | | Dennis Quan | 1 |
| | | R. L. Sendall | 1 |
| Martin-Marietta Corp. | Orlando FL 32805 | John Sura | 2 |
| McDonnell-Douglas Aircraft Co. | St. Louis, MO 63166 | J. F. Reilly | 2 |
| MIT Lincoln Lab | Lexington, MA 02173 | L. B. Anderson | 1 |
| Raytheon Corporation | Bedford, MA 01730 | A. E. Franz | 2 |

END

FILMED

11-85

DTIC